Position identification of spotted hyena (Crocuta crocuta) tracks using different methods of data recording and features extraction

Auteur : Deflandre, Nicolas
Promoteur(s) : Lejeune, Philippe; 2967
Faculté : Gembloux Agro-Bio Tech (GxABT)
Diplôme : Master en bioingénieur : gestion des forêts et des espaces naturels, à finalité spécialisée
Année académique : 2016-2017
URI/URL : http://hdl.handle.net/2268.2/2985

LIÈGE université
Gembloux
Agro-Bio Tech

POSITION IDENTIFICATION OF SPOTTED HYENA (*CROCUTA CROCUTA*) TRACKS USING DIFFERENT METHODS OF DATA RECORDING AND FEATURES EXTRACTION

DEFLANDRE NICOLAS

TRAVAIL DE FIN D'ETUDES PRESENTE EN VUE DE L'OBTENTION DU DIPLOME DE MASTER BIOINGENIEUR EN GESTION DES FORETS ET DES ESPACES NATURELS

ANNEE ACADEMIQUE 2016-2017

CO-PROMOTEURS: LEJEUNE P., MARCHAL A.

LIÈGE université
Gembloux
Agro-Bio Tech

POSITION IDENTIFICATION OF SPOTTED HYENA (*CROCUTA CROCUTA*) TRACKS USING DIFFERENT METHODS OF DATA RECORDING AND FEATURES EXTRACTION

DEFLANDRE NICOLAS

TRAVAIL DE FIN D'ETUDES PRESENTE EN VUE DE L'OBTENTION DU DIPLOME DE MASTER BIOINGENIEUR EN GESTION DES FORETS ET DES ESPACES NATURELS

ANNEE ACADEMIQUE 2016-2017

CO-PROMOTEURS: LEJEUNE P., MARCHAL A.

ACKNOWLEDGMENTS

This Master thesis would not have been possible without the help and support from many people and organisations. I would particularly like to express my gratitude to:

- My two thesis supervisors, Philippe Lejeune and Antoine Marchal, for the support and trust they have given me through the entire project. A particular thanks to Antoine, for his welcome in South Africa and his guidance through the whole experience.
- The Ezemvelo KZN Wildlife agency and the research team of Hluhluwe-iMfolozi Park, especially Dave Druce and Geoff Clinning, for their warm welcome and help in organizing my field work, and Eric Khumalo and Joseph Dlamini, for watching my back while working in the field.
- Le Centre pour le Partenariat et la Coopération au Développement (PACODEL) for financing my plane ticket to South Africa, and Lindsay Lebeau for assisting in the paper work.

- All the researchers, both from the Forestry Department of Gembloux Agro-Bio Tech and from elsewhere, who have helped me with the computer-related and statistical aspects of this thesis: Michel Claereboudt, Emma Sheratt, Yves Brostaux, Adrien Michez, Jonathan Lisein, Stéphanie Bonnet, Samuel Quevauvillers, Vincent Leemans, Zoe Jewell, and the *Panthera* volunteer team.
- All my family, for their financial and moral support, and for not having given up on me after the few hic-ups encountered through my academic career.
- Pierre-Yves, who no matter the circumstances, has always believed in me, guided me in the right direction, and kept me on the right tracks during more difficult times.
- The Gembloux Family, for all the experiences lived in this good old Alma Mater. May she stand for many more years, for many more students. Special SUR LA ROUTE to all the Barmen, and many Bisounous kisses to the Comité 2015.
- Hermione and Nesquick, for having provided me with their companionship and relaxing purring.

To all, including the ones that I have unintentionally forgotten, I thank you for having made me who I am today. But there is one person without who I would definitely not be here. And this person no one else than my life partner. Emily, I would have never come anywhere close to where I am today if it wasn't for you. Our adventure has started five and a half years ago already, but yet it is only beginning. To the many journeys that we will experience together, along with our mischievous fluffy monster!

“It always seems impossible until it is done”

- Nelson Mandela

ABSTRACT

At a time when a sixth mass extinction is about to hit our planet, protection and conservation strategies are the best chances of survival of some wildlife populations. But for those strategies to be effective, the use of reliable monitoring techniques is essential to assess the distribution, dynamic and status of the targeted species. Considering the cost of direct observations and that of invasive high-tech tools, such as camera traps and GPS, collars can be, the use of tracks is a low-cost non-invasive alternative to study elusive species such as carnivores.

In the present study, we evaluate the possibility of identifying the anteroposterior (front or hind) and mediolateral (right or left) position of spotted hyena tracks from their digital models created from field photography. Several combinations of data recording and feature extraction methods were tested so that we could compare the accuracy of prediction of their identification algorithm and determine which combination is the most reliable.

Track sampling, which consisted of photographing encountered tracks, took place in Hluhluwe-iMfolozi Park, in South Africa. 2D and 3D models of 80 tracks (20 from each position) were constructed using *ImageJ* and *Photoscan* software respectively. Landmarks were digitized on the models so that different types of measurements could be extracted by conducting either traditional or geometric morphometrics. Using extracted morphological features, Linear Discriminant Analyses (LDA) generated identification algorithms for each combination of methods. In total, the algorithms of 31 different scenarios were compared, each of which involved (i) a type of model (2D or 3D), (ii) a feature extraction method (traditional or geometric morphometrics), (iii) the types of landmarks used to characterize the form of the models (fixed, fixed and curve-sliders, or fixed and curve- and surface-sliders), (iv) a type of object on which statistical analyses were conducted (independent pads or entire track) , and (v) a type of variables taken into account by the algorithms (shape, size, or both).

Nine of the thirty-one scenarios were able to provide algorithms with accuracies of prediction > 95%. It appeared that the relative position of the pads within a track (i.e. the information provided by the “entire track” objects) as well as their sizes are two pieces of information that are essential for the position identification of spotted hyena track. However, before being able to establish which type of model and which type of landmarks provide the most accurate algorithm, the manipulator bias of each method should be quantified and used as a second evaluation criteria. The track modelling process should also be made more effective both in term of time and manipulator bias.

Keywords: tracks; digital 2D model; digital 3D model; traditional morphometrics; geometric morphometrics; position identification of tracks; ecological monitoring; spotted hyenas; *Crocuta crocuta*.

RÉSUMÉ

Face à la sixième extinction massive qui s'apprête à frapper notre planète, les meilleures chances de survie des populations animales sauvages sont les stratégies de protection et de conservation mises en place par l'Homme. Mais pour que ces stratégies soient efficaces, il est nécessaire que les techniques de suivi des populations soient robustes et fiables. Considérant le coût et la sensibilité des outils technologiques tels que les colliers GPS et caméra-pièges, l'utilisation des traces comme nouvelle technique de monitoring non-invasive et bon marché est de plus en plus étudiée.

Cette étude a pour but d'évaluer la possibilité d'identifier la position antéropostérieure (avant ou arrière) et médiolatérale (gauche ou droite) d'empreintes d'hyènes tachetées à partir de leurs modèles digitalisés. Plusieurs combinaisons de méthodes de récolte et d'extraction de données ont été appliquées afin de comparer la précision de leurs algorithmes d'identification et de déterminer laquelle est la plus fiable.

Les données ont été récoltées à Hluhluwe-iMfolozi Park, en Afrique du Sud. Sur toutes les traces échantillonnées, 80 (20 pour chaque position) ont été modélisées via les logiciels ImageJ (2D) et Photoscan (3D). Après y avoir positionné des points de repères caractérisant leur forme, différents types de mesures ont pu être extraites, soit par morphométrie traditionnelle, soit par morphométrie géométrique. A partir de ces données, des Analyses Discriminatoires Linéaires (ADL) ont généré des algorithmes d'identification pour chaque combinaison de méthodes appliquées. Au total, les algorithmes de 31 scénarios ont pu être comparés, chacun d'eux impliquant (i) un type de modèle (2D ou 3D), (ii) une méthode d'extraction de données (morphométrie traditionnelle ou géométrique), (iii) une combinaison de types de points de repère caractérisant la forme des modèles (fixes, fixes et glisseurs sur courbe, fixes et glisseurs sur courbe et surface), (iv) un type d'objet sur lequel les analyses statistiques étaient appliquées (coussinets indépendants ou empreinte entière), et (v) un type de variables prises en compte par l'algorithme (la configuration, la taille ou les deux).

Sur les 31 scénarios, 9 ont fourni des algorithmes d'une précision supérieure à 95%. La position relative des coussinets au sein d'une empreinte (i.e. l'information contenue dans l'objet « empreinte entière ») et la taille de cette dernière semblent être deux informations essentielles à l'identification de la position d'une empreinte d'hyène tachetée. Cependant, avant de pouvoir déterminer quel type de modèle et quels types de points de repère procurent les meilleurs algorithmes d'identification, il est nécessaire de quantifier les biais engendrés par différents manipulateurs, et de les utiliser comme second critère d'évaluation des méthodes. Le processus de modélisation des traces devrait également être améliorés, notamment au niveau du temps et du biais de manipulateur.

Mots-clés : empreintes ; Modèle 2D ; Modèles 3D ; morphométrie traditionnelle ; morphométrie géométrique ; identification de la position d'empreintes ; monitoring écologique ; hyène tachetée ; *Crocuta crocuta*.

TABLE OF CONTENTS

LIST OF FIGURES

LIST OF TABLES

LIST OF ABBREVIATIONS

Csize	Centroid size
EKZNW	Ezemvelo Kwa-Zulu Natal Wildlife
FIT	Footprint Identification Technique
GM	Geometric Morphometrics
GPA	Generalized Procrustes Analysis
HiP	Hluhluwe-iMfolozi Park
LDA	Linear Discriminant Analysis
MP	Main Pad of a track
PCA	Principal Components Analysis
PC	Principal Components
PS	Photoscan
T1	Toe 1 of a track
T2	Toe 2 of a track
T3	Toe 3 of a track
T4	Toe 4 of a track
TM	Traditional Morphometrics
TPS	Thin-Plate Spline

1 INTRODUCTION

The term “biodiversity” refers to the variety of life forms present in a habitat (Mushegian, 2017). It can be defined by the biotic and abiotic components of the environment, as well as by the interactions within and between the two components. “Every species is unique in its combination of evolutionary history and ecological role” (Mushegian, 2017). This implies that the loss of one inevitably weakens the environment to which it belongs by decreasing the efficiency of its many ecological functions. In spite of these sensitive phenomena, human civilisation keeps expanding, especially in remote underdeveloped areas. This results in massive biodiversity through the destruction of many natural habitats. To counter the impact of human activities, an increasing number of zones of biological importance are given a protection status (Bertzky *et al.*, 2012). However, it may not be sufficient to guarantee the recovery of animal populations that have already been intensely affected. Protection, conservation and management strategies have to be developed in order to ensure the restoration of the ecological equilibrium there once was. But for those strategies to be effective, it is fundamental to monitor animal populations very closely. Monitoring consists of collecting information on a population in order to assess its distribution, dynamic and status. With the constant development of technology, an increasing number of advanced tools are made available for field scientists. However, most of these tools, such as camera traps and Global Positioning System (GPS) collars, are quite expensive, prone to hardware failure, and happen to affect the behaviour of the studied individuals (Jewell *et al.,* 2016).

Considering those limitations, the use of tracks can be presented as a low-cost non-invasive alternative to study elusive species (species that are rarely seen) such as carnivores. With the right tools, individuals can be identified from their tracks, and their trails (continuous sequences of tracks made by the same individual) can give information about their activity (behaviour) and body condition (Liedenberg, 1990; Heinenmeyer, 2008; Peig and Green, 2010; Marchal et al., 2016). Three main types of research that have used tracks stand out:

- For more than three decades, the ‘pugmark census method’ has been used to censor tigers *Panthera tigris* in India. However, it has been highly criticized (Karanth *et al.,* 2003), notably for the misidentification of the foot from which each track originates. This substantial error led to assigning tracks made by different feet of the same individual to different individual, hence overestimating the actual population.
- The Footprint Identification Technology (FIT) is a software created by the non-profit organization *WildTrack*. By extracting morphological features such as distances and angles from two-dimensions (2D) images of tracks, their research teams have already developed identification algorithms for several species, such as black and white rhinoceros (*Diceros bicornis* and *Ceratotherium simum* respectively*)*, cheetah (*Acinonyx jubatus*), mountain lion (*Puma concolor*), and tiger (*Panthera tigris*).
- Marchal *et al.* (2016) have developed another method to identify African lions *Panthera leo* from their tracks: they used photogrammetry, the “science of measuring in photos” (Linder, 2009), to

construct three-dimensional (3D) models of tracks, and applied geometric morphometrics to extract morphological data.

Morphometrics is the study of shape variation and its covariation with other variables (Bookstein, 1991; Zelditch et al., 2012). Traditional and geometric morphometrics are two different approaches, but they both enable the extraction of different types of measurements from any objects (in this case, tracks) (their concepts are explained in Chapter 3.1).

In Hluhluwe-iMfolozi Park (HiP), situated in the Province of KwaZulu-Natal in South Africa, there have been some concerns about a significant decrease in the number of spotted hyenas *Crocuta crocuta* (EKZNW, 2015). The monitoring, behavioural study and health assessment of the current population are therefore urgently needed, hence the park managers' interest in the development of the use of tracks in wildlife research.

Considering the results and criticisms from previous studies on tracks, and from the perspective of using tracks and trails as a monitoring tool, the objectives of this study are as follows:

1) Develop an algorithm that can identify the anteroposterior (front or hind) and mediolateral (right or left) position of spotted hyena tracks from their replicas
2) Test the accuracy of prediction of the position identification algorithms obtained from different methods of data recording (2D versus 3D) and feature extraction (traditional versus geometric morphometrics)

We start this manuscript by explaining the importance of carnivore conservation and the interest in the use of tracks as a monitoring method. The evolution of morphometrics, the comparison between its traditional and geometric approaches, and the general concepts of the latter are explained in Chapter 3, before a brief description of the species of interest, the spotted hyena, in Chapter 4. The objectives of the study and the methodology, from the track sampling protocol to the statistical analyses conducted on the models of the track variables, are covered in Chapters 5 and 6. The results are presented in Chapter 7 and analysed in Chapter. Finally, we discuss a few ideas to improve the modelling process of tracks, both in term of time and manipulator bias, and introduce perspectives of tracks in future wildlife studies.

2 CARNIVORES CONSERVATION AND MONITORING

2.1 The importance of carnivore conservation

Within the context of conservation, species are classified into one or several of the following categories (Caro, 2010):

- Flagship species, which tend to attract more attention from the general public;
- Indicator species, which are used to estimate the ecological status of an environment;
- Keystone species, which exert a fundamental role in an ecosystem;
- Umbrella species, which require large areas, whose protection hence benefit other species;
- Threatened species, which are those more prone to extinction.

Any species that fit into at least one of these categories are called surrogate species. They are used "to represent other species or aspects of the environment to attain a conservation objective" (Caro, 2010).

As a matter of fact, most large carnivore species match several of these labels: (i) many of them, such as the "African big cats" (lion, cheetah, and leopard (*Panthera pardus*)), are some of the main tourist attractions (flagship species); (ii) being at the top of the food chains, they regulate herbivore populations through predation (Ripple and Beschta, 2012), as well as meso-carnivore populations through intra-guild competition (Ritchie and Johnson, 2009, Ripple *et al.*, 2014) (keystone species); (iii) because they feed on other animals, their geographical range is larger, and therefore include other species' range (umbrella species); and finally (iv) their low population density makes them more vulnerable (threatened species): if the number of individuals in a population is too low, the genetic diversity may not be high enough, which would lead to a high consanguinity rate that will jeopardize the health of the future generations.

Because carnivores are particularly important in the context of conservation (Gittleman *et al.*, 2001), so is the monitoring of their population. Hence the necessity to access effective and reliable monitoring tools.

2.2 Monitoring methods

Monitoring methods can be classified into two categories: invasive and non-invasive. A non-invasive method does not require the studied animal to be directly observed or handled by the researcher (MacKay *et al.*, 2008), whereas an invasive one involves a direct contact, and therefore presents a potential effect on its behaviour and health.

However, the distinction between these two types of methods is not that straightforward. Camera traps, for instance, are considered to be non-invasive, but their flashes can result in trap shyness (Wegge *et al.,* 2004; Schipper, 2007). And the mere presence of the equipment that carries human smell can by itself disturb wildlife (MacKay *et al.,* 2008).

New technologies, such as infrared camera trap, may solve some of these issues. But high-tech equipment is expensive, prone to hardware failure (low batteries, damageable by animals) and can be stolen. Jewell *et al.* (2016) pointed out other limitations linked to these techniques (limited range of camera traps, for instance), as well as the fact that the estimates they produce happen to differ quite significantly from each other, especially for wide-ranging and elusive species such as carnivores. For instance, estimates of the cheetah population density in Namibia vary from 2.5 (± 0.73) cheetahs/1,000 km^2 using radio telemetry to 4.1 (± 0.4) cheetahs/1,000 km^2 using camera trapping (Marker *et al.,* 2007).

These limitations highlight the necessity to develop a robust, cost-effective and flexible tool for monitoring endangered species (Jewell *et al.,* 2016).

Tracks present a good alternative. The animals do not need to be captured, nor even directly observed; their tracks are more easily spotted than the animals themselves; and if correctly identified, tracks are the best proof of the presence of certain species in an area (Liebenberg, 1990; Marchal, 2017).

2.3 Tracking

2.3.1 History

The art of tracking is not only about looking at, recognizing or following tracks; it also involves a general awareness of the environment, the use of senses of smell and hearing, and the ability to recognize signs other than tracks (Gutteridge and Liebenberg, 2013). It may have been the first creative science that was practiced by the earliest members of anatomically modern *Homo sapiens* (Liebenberg, 1990).

Nowadays, the San People from the Kalahari Desert of southern Africa continue to apply the art of tracking through the practice of persistence hunting, which consists of running down a prey to exhaustion during the hottest temperatures of the day (Liebenberg, 2006). Their tracking abilities have even been of some use for behavioural ecology studies of large carnivores (Eloff, 1984; Bothma and Le Riche, 1984).

Although the accuracies of their tracking skills are impressive (100% for species identification of herbivores and carnivores, and more than 90% for age, sex and individual identification of three carnivore species – Stander *et al.,* 1997), track recognition remains subjective and is hardly applicable by non-experienced trackers. It is therefore worth looking into developing the study of tracks as a more objective approach, in order to expend its use to a scientific level.

2.3.2 Tracks and trails as a monitoring tool

A track can be defined as the impression of a foot, or a paw, on a surface. Synonyms found in the literature are footprint, pawprint, pugmark, or spoor (Jewel *et al.*, 2016; Marchal, 2017). It represents the signature and evidence of the passage of an animal that is no longer visible (Liebenberg, 1990).

The foot anatomy varies between species, but also within a species (Liebenberg, 1990). For instance, because males are usually bigger than females, so are their feet and tracks. Like the fingerprints of human beings, each individual's track differs in subtle ways. Hence the possibility, in principle, to identify an individual from its tracks (Liebenberg, 1990).

If characteristics such as sex, age, and even the identity of an individual can be recognised from its tracks (Jewel *et al.,* 2016), it should then be possible to study the demography of a population, and even monitor its individuals independently. The behaviour of an individual can also be studied from a sequence of its tracks (i.e. a trail). The gait of an animal is the way in which the animal is moving, so its trail can be seen as the signature of the gait recorded into the substrate.

Because the relative position of tracks mainly depends on the anatomy, the behaviour, and the speed of the animal (Liebenberg, 1990), the characteristics of a trail (such as measurements between each track) could be registered and linked to its particular gait (Marchal, 2017). This would then allow scientists to identify and study the behaviour of an individual by simply analysing its tracks and trails.

However, in order to study the relative position of tracks within a trail, it is necessary to correctly identify the foot (i.e. paw) from which each track originates. Hence the main objective of this study: to develop an algorithm that can objectively identify the position of a track (front or hind and right or left).

2.3.3 The use of tracks in recent studies

Various studies on large carnivores have indicated that it is possible to use tracks to identify the species, sex and identity of individuals (Jewell *et al.,* 2016). The use of tracks can be divided into three categories, which present an increasing level of complexity (Marchal, 2017): track identification, track count, and track measurements.

2.3.3.1 Track identification

Track identification is a qualitative approach that involves the comparison between a drawing or a photograph of a track from a tracking book (e.g. Liedenberg, 1990) and an actual track. The advantage is that anyone who is simply passionate about wildlife can use it. However, this method of track recognition is very subjective, and the risk of misidentification is too high for it to be scientifically acceptable.

The “pugmark census method” is one of the most significant examples of track use in wildlife monitoring. For more than thirty years, thousands of rangers were regularly searching for tiger tracks across India. Once recorded (either using plaster casts or tracings), the track replicas were compared to subjectively discriminate the different individuals, and thus estimate the national population size. This method, however, was highly criticized for various reasons (Karanth *et al.,* 2003; Marchal, 2017), including the misidentifications of the paw from which the track originates. Because tracks made by different feet of a same individual were actually assigned to different individuals, the population has been over-estimated (Karanth *et al.,* 2003; Marchal, 2017).

2.3.3.2 Track count

By counting the number of tracks detected per unit of sampling effort (e.g. plots or transects), an index of relative abundance can be calculated (Wilson and Delahay, 2001). This type of index can be used to study the trend of a population size over time, or compare population sizes from different areas (Wilson and Delahay, 2001).

Stander (1998) studied the efficiency of track count as an inventory method. He independently compared the track frequency along transects with the true density of lions, leopards, and wild dogs (*Lycaon pictus*), thus providing a calibration factor. However, as Stander (1998) explained, indices of relative abundance highly depend on the sampling effort, the type of habitat, and the road density. Furthermore, the degradation time of the tracks depends on the season, type of substrate and topography. Considering that the longer it takes for a track to be degraded, the more likely it is to be detected, we can assume that the values of the index may also be affected by those three environmental factors. Finally, as for the previous category of track use, track count also requires the correct identification of the tracks that are taken into account. So in order to limit the risk of over- or under-estimations, only expert trackers should be in charge of collecting data.

2.3.3.3 Track measurements

With the aim of creating a more objective and quantifiable method of track identification, indigenous trackers and tracking books have been replaced by track measurements and multivariate analyses. The measurements can be recorded in two ways: (i) directly on the tracks by using a calliper, or (ii) on their replicas, such as drawings or photographs. The first option poses a higher risk of destroying the tracks and limits the number of measurements that can be recorded (Marchal *et al.,* 2016). Furthermore, it can be quite time consuming, which is not ideal considering the dangers one can come to face in the wilderness. On the other hand, measurements extracted from digitalized pictures were proven to be more precise and less prone to manipulator bias than if they were made directly on the track (Muñoz-Muñoz and Perpiñán, 2010).

2.3.3.3.1 Two- or three- dimensional replicas of tracks

Up until recently, all the studies were using 2D-images (drawings and photographs) as track replicas. For instance, the non-profit organization “WildTrack”, founded by Zoe Jewell and Sky Alihai, from

Duke's University, has developed a software named "The Footprint Identification Technology" (FIT). It uses digital images of tracks to create an algorithm that can identify the species and individual identity from tracks. The relative simplicity of the sampling protocol (only one picture overhead the print) enables citizen scientists, field practitioners and community members to collect and send images to the research team. The 2D-analysis of tracks has generated valid individual identification algorithms for rhinoceros (Law *et al.,* 2013), mountain lions (Jewell *et al.,* 2014), Amur tigers (*Panthera tigris altaica*) (Gu *et al.,* 2015), and cheetahs (Jewell *et al.,* 2016).

However, sampling techniques that are limited to 2D can present some limitations. For instance, external factors such as soil components (which influence the depth and shape of the track; Liebenberg, 1990) are not taken into account, and the parallax error (which occurs if the camera is not aligned directly over the object) may lead to significant variations in the datasets (Mullin and Taylor, 2002). Furthermore, most of WildTrack's studies were conducted on captive animals. Thanks to ideal sampling conditions, the quality of the tracks was excellent, which is rarely the case in the wilderness.

The use of 3D-modelling inevitably provides a better representation of reality (Marchal *et al*., 2016). Marchal *et al.* (2016) have shown that close-range digital photogrammetry is an efficient tool to produce 3D reconstruction of tracks. The sampling protocol consists of taking eight to fifteen photographs from different angles and distances, but using the same focal length. It may seem more complex than the use of 2D, but since depth is taken into account, it provides more data and therefore a more realistic replication of the tracks. It is thus expected that it will "enable the correct identification of more individuals on a greater variety of substrate with fewer tracks required per individual" (Marchal *et al.,* 2016).

2.3.3.3.2 Photogrammetry and extraction of measurements

Photogrammetry is a method used to collect quantitative information of an object, such as distances, areas and volumes, without involving any physical contact to it (Linder, 2009). Its principle is the same as the human vision: by getting two different images (one from each eye), the brain allows us to see objects in a spatial manner. In the same way, specialized computer software can create, from minimum two photographs of the same object, a 3D representation of the object.

The method used to extract measurements from the model of an object (in this case, a track) is morphometrics, which literally means the measure (*metrics*) of form (*morph*). Up until recently, the majority of studies have used variables such as distances, angles and areas. But a new approach, based on the coordinates of landmarks that are positioned on the models, allows the quantification of shape independently from its size.

The next chapter, "Morphometrics", describes and compares those different approaches.

3 MORPHOMETRICS

3.1 History

3.1.1 From morphology to traditional morphometrics

Morphology is defined as the study of forms and structure of organisms (Oxford University Press, 2017). It is a branch of biological science used to qualitatively describe organisms. The differences in shape can be summarized by comparing them to more familiar forms and objects, such as circles or letters of the alphabet (Zelditch *et al.,* 2012). Although this approach helps to visualize the object of interest, it does not procure precise measurements. The information that is extracted happens to be vague, inaccurate, and even misleading, especially when the shapes are more complex.

During the 20th century, thanks to advances in statistics, scientists started studying the variations in form of organisms between biological groups. This quantitative analysis of shape variations is called morphometrics (Zelditch *et al.,* 2012). The application of multivariate analyses on the measures of distances was a first quantitative approach to the study of forms, and is now known as "traditional morphometrics" (Mitteroecker and Gunz, 2009).

3.1.2 From traditional to geometric morphometrics

The datasets provided by traditional morphometrics consists of a list of measurements between anatomical loci. Because several of these measurements radiate from a same point, many of them overlap and run in similar directions (Zelitch *et al.,* 2012). The information they procure is therefore redundant, and is at risk of being affected by any error in locating that one common point. Furthermore, the measurements extracted by traditional morphometrics are all of size (length, width, and depth), which means "the original geometric relationship among the points may not be reconstructable" from a sample of those measurements (Mitteroecker and Gunz, 2009). The geometry of the object is therefore underestimated, and its representation can only be partial (Cuchi *et al.*, 2015).

In the 1980s, the invention of coordinate-based methods and the discovery of statistical theory of shape brought a new dimension to morphometrics (Mitteroecker and Gunz, 2009). "Geometric morphometrics" involves statistical analyses based on landmark coordinates (Mitteroecker and Gunz, 2009), which are used to record relative positions of morphological points, curves and surfaces in order to quantify shape (Adams *et al.,* 2013).

3.2 Concepts of geometric morphometrics

Two main characteristics define geometric morphometrics (Mitteroecker and Gunz, 2009): (i) the preservation of the geometry of landmark configurations throughout statistical analysis, which allows to (ii) analyse and represent statistical results of shape and size variations independently from one another. The concept of size and shape has been much contested over the history of morphometrics. The main reason is probably due to the fact that "size" has many different definitions (Zelditch *et al.,* 2012). This is why it is important to understand the following concepts of geometric morphometrics.

3.2.1 Form, shape, and size

Morphometrics come from the Greek *metron*, measurement, and *morph*, form. The term "form" incorporates both the shape and size of an object. The relations between these three terms can be summarized by Equation 1 (Mitteroecker and Gunz, 2009; Zelditch *et al.,* 2012; Cucchi *et al.,* 2015).

$$Form = Shape + Size \Leftrightarrow Shape = Form - Size \qquad \text{Equation 1}$$

In traditional morphometrics, the size does not have a standard definition, as it can be defined by different parameters, such as length, perimeter and surface. The distinction between shape and form is therefore not relevant.

In geometric morphometrics, shape is defined as all the geometric information that is independent from the size, location and orientation of the object (Mitteroecker and Gunz, 2009). The shapes of two or more objects can be compared once all the differences that are related to those three factors are filtered out. The Procrustes superimposition (Section 3.2.3) is the most widespread method used to do so, as its mathematical and statistical properties are best understood (Bookstein, 1996).

The shape of an object is characterized by the Procrustes coordinates of its landmarks (which are initially positioned in a way that best symbolizes the shape; Section 3.2.2). Its size is defined by the centroid size (Csize), which corresponds to the centre of gravity of the landmarks. The coordinates of the centroid are the average of those of the landmarks, and its value is given by Equation 2, in which a, b, c and d are the distances between the centre of gravity and each of the four landmarks (Figure 1).

$$Csize = \sqrt{a^2 + b^2 + c^2 + d^2} \qquad \text{Equation 2}$$

Shape and size are still closely related to one another (Mitteroecker and Gunz, 2009), as the shape's variability of an object often increases with its size. However, their separation does not involve a loss of information about that relation (Zelditch *et al.,* 2012). It is indeed relatively easy to analyse the latter through conventional statistical methods.

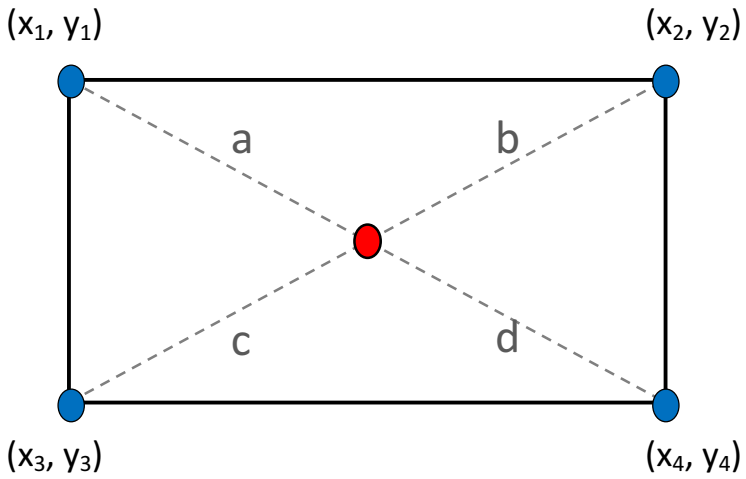

Figure 1 - *The centroid (in red) and landmarks (in blue) of an object. The size of the centroid is calculated using Equation 2. The letters a, b, c, and d represent the Euclidean distances between the centroid and each of the landmark.*

3.2.2 Landmarks

The most effective way to analyse the form of an object is by recording the geometric locations of landmark points (Bookstein, 1991). Landmarks are "biologically homologous anatomical loci whose names (such as 'bridge of the nose' or 'tip of the chin') are intended to imply biological correspondence from form to form" (Zelditch *et al.,* 2012). In other words, "landmark points have the same locations in every other form of the study" (Bookstein, 1991).

In geometric morphometric, each object is symbolized by the configuration of its landmarks. A configuration is a reference system in which the coordinates represent a unique object, which contains all the information on size, shape, location and orientation (Zelditch *et al.,* 2012). It is the configurations of landmarks that are measured and analysed through geometric morphometrics.

Bookstein (1991) has classified the landmarks into three categories: type 1, type 2 and type 3. The first category includes the landmarks that have a precise anatomical definition (for instance, the intersection of several elements). The second type accepts the landmarks that are defined by geometrical criteria, such as the extremities of a structure. The landmarks from the last category are those that are constructed by the manipulator, and should therefore not even be considered as landmarks.

3.2.3 Procrustes superimposition

The most common method to isolate information on shape is the Procrustes superimposition (Bookstein, 1996). It consists of superposing two or more configurations of landmarks using a least-squared oriented approach that involves three steps (Mitteroecker and Gunz, 2009):

1) Translation of the landmark configurations of all specimens until they share the same centroid (i.e. the effects of position are removed)
2) Scaling of the landmark configurations so that they all have the same centroid size. (i.e. the effects of size are removed)
3) Rotation of the configurations around their centroid until the sum of squared Euclidian distances between the homologous landmarks is minimal. For more than two forms, this rotation step is an iterative algorithm named Generalized Procrustes Analysis (GPA).

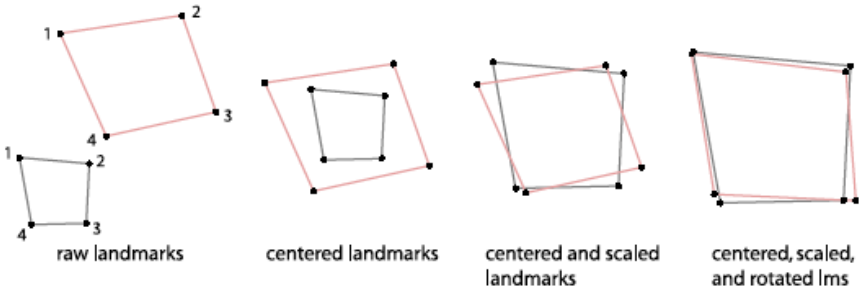

Figure 2 - *The three steps of the Procrustes superimposition: translation to a common origin (centered landmarks), scaling to unit centroid size (centered and scaled landmarks), and rotation to minimize the sum of squared Euclidean distances among the homologous landmarks (centered, scaled, and rotated lms) (Mitteroecker and Gunz, 2009).*

Mitteroecker and Gunz (2009) define the following concepts:

- The "Procrustes coordinates" are the coordinates of each landmark that result from the Procrustes superimposition. They represent the "Procrustes configuration" of a specimen.
- The "consensus configuration", or average configuration, is the average shape of all the specimens. Its sum of squared distances to the other shape is minimal, and is thus the maximum likelihood estimate of the mean.
- The "Procrustes residuals" of a specimen are the differences between the average configuration and the Procrustes configuration of that specimen.
- The "Procrustes distance" is the Euclidean distance between the Procrustes configurations of two specimens.

As the three steps of the Procrustes superimposition remove the effects of size, position, and orientation, the geometry of the configurations is preserved through the analyses. This allows the acquisition of statistical results on the actual shape of the object as well as their graphical representations.

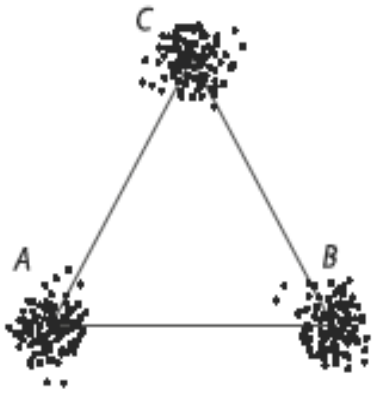

Figure 3 - *The consensus configuration (black line) of a hundred random triangles whose vertices (black dots) are the Procrustes coordinates (Mitteroecker and Gunz, 2009).*

3.2.4 Semi-landmarks

Besides the three types of landmarks categorized by Bookstein (1991; see Section 3.2.2), three important criteria define a set of ideal landmarks (Zelditch *et al.,* 2012): (i) the landmarks are homologous between each specimen (i.e. the points on one specimen correspond to that point on all individuals), (ii) they provide adequate coverage of the morphology of the object (i.e. they are evenly spread across the object), and (iii) they can be found repeatedly and reliably (i.e. no matter how many times and how many different manipulators position the landmarks on a same object, the variability of the coordinates should be insignificant).

However, many applications do not always meet all these requirements. On long curves or large surfaces, such as the back of a skull for instance, only a few homologous points, if not none, can be precisely located repetitively on each specimen.

In such situations, one must content with semi-landmarks, or sliding-landmarks. From one specimen to another the Procrustes superimposition allows the landmarks to "slide" along the curve or surface to which they belong, until some measure of shape difference among the configurations is minimized (Mitteroecker and Gunz, 2009). Semi-landmarks are therefore not homologous (Zelditch *et al.,* 2012), but in order for the algorithm to work, the structure (curve or surface) to which they belong has to be (Mitteroecker and Gunz, 2009).

3.2.5 Graphical visualization

The preserved geometry of the configurations allows graphical representations of shape differences and variations between specimens. Two types of visualisation exist (Adams *et al.*, 2013; Cucchi *et al.,* 2015):

- Landmark displacement, which consists of simply observing the differences (represented by points or vectors) between the coordinates of two sets of homologous landmarks;
- Deformation grids, which involve a "Thin-Plate Spline" interpolation function (Section 3.2.5.1).

3.2.5.1 Thin-Plate Spline (TPS)

The main goal of a TPS function is to "visualize the shape difference between one reference form and one target form, based on a set of homologous point coordinates measured on both forms" (Gunz and Mitteroecker, 2013). The template configuration is represented by a square grid, which the TPS algorithm deforms in a way that the measured points match their counterparts from a target configuration (Figure 4). The space in-between the landmarks is interpolated as smoothly as possible (Gunz and Mitteroecker, 2013), which is realized by minimizing the bending energy of the deformation. The "bending energy" is a measure of the amount of local shape deformation; it is "a scalar quantity computed as the integral of the squared second derivatives of that deformation"

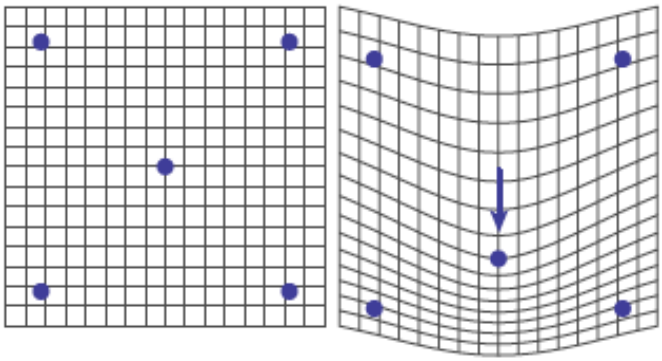

Figure 4 – *Schematic of a Thin-Plate Spline (TPS) deformation. The template configuration is on the left and the target configuration on the right. The blue dots represent five landmarks. The deformation grid on the right illustrates the thin-plate spline function between these configurations as it has been applied to the left regular grid. It is a visualization of the differences between the two shapes. (Mitteroecker and Gunz, 2009)*

(Mitteroecker and Gunz, 2009).

The deformed grid that results from the TPS function illustrates how the template configuration should be stretched or compressed in order for it to match the target shape (Gunz and Mitteroecker, 2013).

4 SPOTTED HYENA

Although the spotted hyena looks like a large canid, it makes up, along with the aardwolf (*Proteles cristalus*), brown hyena (*Parahyaena brunnea*) and striped hyena (*Hyaean hyaena*), its own biological family *Hyaenidae* within the order *Carnivora*.

With a total world population of 10,000 mature individuals, the spotted hyena (hereafter, hyena) remains widespread in Sub-Saharan Africa (Bohm and Höner, 2015). They are present in many different types of habitats, such as semi-desert, savannah, and both open and dense dry woodlands, and may be found at lower densities in extreme desert conditions, tropical rainforests, and high mountains (Bohm and Höner, 2015).

Figure 5 - *Distribution of the spotted hyenas in Africa (Bohm and Höner, 2015)*

They have therefore been labelled as “Least Concerned” in the Red List of Threatened Species of the IUCN (International Union for Conservation of Nature). However, outside protected areas, and even within some of them, there is a continuing decline in populations. This is mainly due to persecution and habitat loss. In some countries for instance, when hyenas are known to have preyed upon livestock, the authorities allow local residents to kill them (Bohm and Höner, 2015). In fenced protected areas, such as the one in which this study was conducted (see Section 6.1), the risk of inbreeding is higher, which results in low fitness and survival rate of the new generations.

Heynas form permanent complex social groups called clans, whose size and territory range vary depending on prey abundance (Holekamp *et al.*, 2007). In the vast prey-rich plains of eastern Africa for instance, a clan often contains more than 70 individuals (Kruuk, 1972). Adult females, who weight between 44 and 64 kg, dominate the males, who are smaller (40 to 55 kg). As for most mammals, most of their weight is concentrated in their upper body (thoracic cage, head with powerful jaws). As a probable result of evolution, their front paws are larger, in order to prevent them from sinking in softer soils (same idea as using snowshoeing for hiking in snow) (Liebenberg, 1990; Gutteridge and Liebenberg, 2013).

As males disperse voluntarily from their natal groups after puberty (Holekamp et al., 2007), the core of a clan is usually composed of several matrilines. However, individuals spend much of their time alone or in smaller groups, especially when foraging: the probability of making a successful kill increases by approximately 20% with the presence of each additional hunter (Holekamp et al., 2007), but competition between hyenas from different matrilines (although from a same clan) is often pretty intense around a carcass (Holekamp *et al.*, 2007).

Although people tend to think hyenas are scavengers, most of their diet actually consists of preys they hunt down themselves (Kruuk, 1972; Trinkel and Kastberger, 2005). With their front legs that are longer than their back legs and a heart that is twice the size of the one of a lion, they are built for stalking and chasing their preys for many miles (Kruuk, 1972). Lions, on the other hand, happens to scavenge the preys of hyenas more often than the other way around (Trinkel and Kastberger, 2005). The large degree of dietary overlap between the two species inevitably leads to kleptoparasitism and intra-guild competition (Hayward *et al.,* 2015). Although it is one of the natural ways of regulating animal populations, it may rapidly have too much of a negative impact in the case of a fenced area, as the clans do not have the possibility to find new territories with less competition.

To collect information about the feeding habits, competition and impact of the human-wildlife conflict, tracks can be of some use. The species (and even the individuals, if their tracks have already been recorded) responsible for the kill or involved in a conflict can be objectively identified by analysing the tracks around the carcass.

The particular morphology of hyena legs gives them a very distinctive walk. The species can therefore easily be identified by its normal trail (Figure 7, Section 6.2), but as explained earlier, trails vary with the gait of the individual. The correct identification of the later, or even the species or track position, can therefore rapidly be compromised. Hence the necessity of developing a scientifically approved method that will allow the objective identification of tracks in every possible situation.

5 OBJECTIVES OF THE STUDY

From the perspective of using tracks and trails as an effective and reliable monitoring tool, the main objective of this study is to assess the possibility of objectively identifying the anteroposterior (front or hind) and mediolateral (right or left) position of spotted hyena tracks.

To achieve this main objective, we tested different methods to record tracks (2D versus 3D) and extract features information (traditional versus geometric morphometrics). For all possible combinations of methods, we developed several algorithms capable of identifying the relative position of tracks, and we compared their accuracies of prediction.

A study with the same main objective was conducted by Marchal *et al.* (2017). They positioned fixed landmarks on 3D-models of lion tracks and extracted information using geometric morphometrics. Through a series of statistical analyses, they obtained a position identification algorithm whose accuracy of prediction was 91.2%.

Because 3D-modelling procures a better representation of the studied object, and geometric morphometrics applies more advanced statistical analyses, we believed that the combination of these two methods, along with the use of different types of landmarks, would provide more accurate identification algorithms.

6 METHODOLOGY

6.1 Study site

South Africa is a country located at the southern tip of the African continent (Figure 6 A). Its total area is 1,219,090 km^2 (forty times bigger than Belgium), and its population, in July 2017, was recorded to be around 54.3 million inhabitants (five times the Belgian population) (CIA,2017).

Figure 6- *Maps of South Africa (A and B) (CIA, 2017) and location of Hluhluwe-iMfolozi iPark in the Province of KwaZulu-Natal (C) (Hluhluwe Game Reserve, 2017)*

Field data were collected in Hluhluwe-iMfolozi Park (HiP), which is located in the eastern Province of KwaZulu-Natal (KZN) (Figure 6.C). The "Hluhluwe Game Reserve" and "iMfolozi Game Reserve", along with "St Lucia Game Reserve", were the oldest game reserves in Africa. They were established in 1895 (Charlton-Perkins and De la Harpe, 1995), and combined in 1989 to form the HiP of today. The park now covers approximately 900 km^2, is fully fenced, and has been managed by the provincial conservation agency Ezemvelo KZN Wildlife (EKZNW) since 2000 (Hluhluwe Game Reserve, 2017).

In spite of the intensive hunting that wiped out most mammal populations during the 19th century (Cromsigt *et al.*, 2017), and thanks to the protection status and management policy that have been put in place since then, HiP now shelters more than 1200 species of plants, 84 of mammals, and 350 of birds (Hluhluwe Game Reserve, 2017). The topography of the park is quite weathered and rocky, with altitudes that range between 40 and 560 meters above sea level. Three rivers (Black iMfolozi, White iMfolozi, and Hluhluwe) traverse the park. The mean annual precipitations range between 650 and 985 mm per year. The main habitat is woodland savannah interposed with shrub tickets, but semi-deciduous forests are also present in the north, and open savannah woodlands in the south (Mucina and Rutherford, 2006).

The most recent study on the hyena population in HiP was led by Graf *et al*. (2009). In 2003 and 2004, the population density was estimated at 0.37 individuals/km^2 by conducting hyena call-ins (Ogutu and Dublin, 1998; Mills *et al.*, 2001). The same method was used again by the research team of HiP in 2010, 2013 and 2015 (EKZNW, 2015; Cromsigt *et al.,* 2017). The hyena population seemed relatively stable from 2003 to 2010, as its density only decreased from 0.37 to 0.34 individuals/km^2.

However, it suddenly plunged to less than half these numbers in 2013 (0.14 individuals/km^2) and 2015 (0.12 individuals/km^2) (Appendix A). Cromsigt *et al.* (2017) believed that this substantial decrease might be due to a possible habituation of the hyenas to the call-in method. However, the time period between each census appeared to be quite considerable (two to six years), and it seems plausible that such a population decrease may be the consequence of an increasing degree of competition with other carnivores. By early 2000 the number of lions and African wild dogs in HiP was less than 70 and 15 individuals respectively. But through re-introductions that were conducted since then, their population grew to around 120 lions and 70 African wild dogs by January 2015 (Cromsigt *et al.,* 2017).

Whether the call-in method is not effective any more or the hyena population is indeed being decimated, a more complete monitoring research needs to be conducted.

6.2 Track sampling protocol

The sampling of hyena tracks was conducted between 13 March and 13 April 2017. To garantee the correct identification of the species whose tracks have been sampled, camera traps (Cuddeback Attack, Green Bay, USA) were set up in certain key-locations: in riverbeds, where track contours are more well-defined (Liedenberg, 1990), and along game paths leading to water points, where animal density is usually higher. To optimize the print quality in this last type of location, track stations in front of the camera traps were prepared as recommended by Jewell *et al.* (2016): 1cm-depth path of natural substrate was smoothed with standard gardening tools. The surface of these prepared plots was long enough to ensure trails of minimum four track sets. In the case of hyenas, a track set consists of a front track followed by the hind track from the opposite side (Figure 7).

Because tracks tend to degrade over time, sampling had to take place within 24 hours. Fieldwork was conducted every morning from 06:00 am to 12:00 pm. It consisted of checking on the camera trap locations and walking along the riverbeds to look for trails left by individuals that would have wandered there during the previous night (spotted hyenas are mainly nocturnal). Additionally, tracks from other species were opportunistically sampled to start a multispecies database of tracks.

Tracks with relatively well-distinguished contours were sampled. They were part of a trail in order to enable the identification of their relative position (front or hind and left or right) (Figure 7). Because the front and hind tracks were usually close to each other, they could not be sampled separately. Each sampling therefore involved photographing a set of two tracks (hereafter, track set). Their separation was one of the step involved in image processing (Section 6.3).

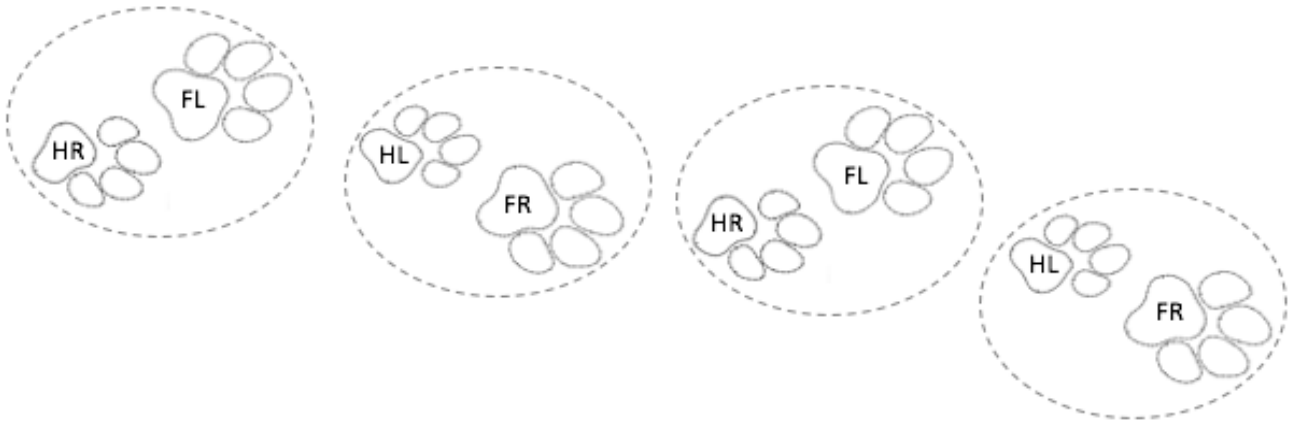

Figure 7 - *Diagram of a spotted hyena trail. The track positions are referred to as FL (Front Left), FR (Front Right), HL (Hind Left), and HR (Hind Right). Each circle represents a track set, which, in the case of spotted hyenas, consists of a front track followed by the hind track from the opposite side.*

Track sampling in 2D requires only one good-quality picture of the track. It has to be taken directly overhead to avoid parallax error (Jewell *et al.,* 2016). To create reliable 3D-model, eight to fifteen photographs, taken with the same focal length from different angles and distances, are necessary (Agisoft LLC, 2016; Marchal *et al.,* 2016).

For the data collection to be as quick as possible, both sampling methods were combined into one. Each set of pictures consisted of (i) one taken directly overhead the track set (for 2D-modelling) and (ii) nine others taken as the manipulator turned around it (Figure 11, Section 6.3.2.1).

To provide a scale and prevent the manipulator to step too close to the track set, we positioned two square rulers around it. They remained motionless during sampling, as they had to appear in at least two pictures (Agisoft LLC, 2016), including the one used for 2D-modelling.

We also recorded the date and time of each sampled track and visually estimated several soil characteristics, such as (i) the substrate (sandy, loamy, or clayey), (ii) the type of soil (game path, riverbed, sandy road or dirt road), (iii) the humidity of the soil (dry, slightly humid, very humid), and (iv) the slope (flat, slight slope or strong slope).

6.3 Image processing

We used the same tracks for both 2D and 3D analyses, but we first had to pre-treat the 2D-images and reconstruct the 3D-models.

6.3.1 Two-dimensional (2D) images

Statistical analyses can be conducted directly on images with jpeg format (hereafter *.jpg), but to assess which pad provides the information that is the most useful for the discrimination of the track positions, the different components of each track first had to be segmented and the curves of their shape digitalized. Such operations can usually be realized using semi-automatic tools, which are

available in most image-processing software. Unfortunately, due to the lack of contrast in terms of colour and texture between the track and unaffected substrate, these segmentation tools were not applicable in this study. Therefore, we had to segment the tracks manually, using the "polygonal selection" tool of the ImageJ software (Schindelin *et al.*, 2012). This manual step represents a constraint to the reliable collection of data, as besides being time consuming, it can lead to a significant variability in the resulting shape of each pad. To limit this bias, a unique manipulator realized the segmentation process.

ImageJ is a software that focuses on biological-image analysis (Schindelin *et al.,* 2012). We used its open-source version Fiji for the pre-treatment of the photographs.

6.3.1.1 Image scaling

The rulers placed next to the tracks during sampling were used to scale the images. We drew a line of twenty centimetres on one of the rulers (Figure 8), so that the "Set Scale" panel could give us the original scale of the picture (116.25 pixels/cm in the example given in Figure 8). To obtain a common scale of 100 pixels/cm for every image, we applied a corresponding ratio on the X and Y scales in the "Scale" panel (in the example given in Figure 8, ratio = 100/116.25 = 0.86). The scaled photograph was then automatically opened in a new window and saved as a new *.jpg image.

We finally verified the scale of the new *.jpg image (100 pixels/cm) in the "Set Scale" panel.

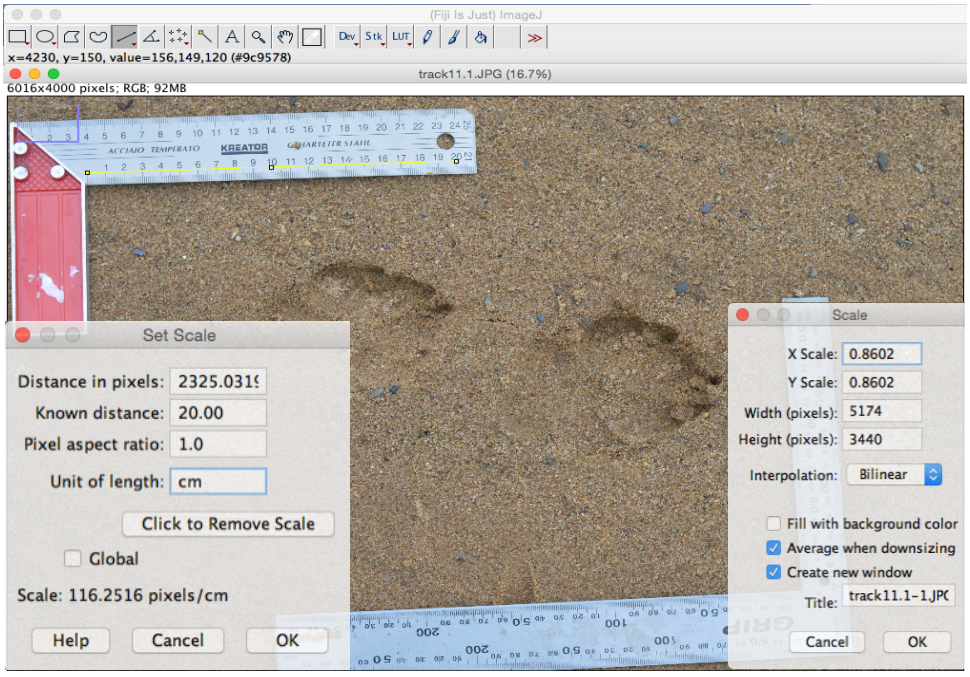

Figure 8 - *Image scaling process in Fiji. A line of 20 cm (in yellow) was drawn with the "Freehand line" tool on one of the ruler. The "Set Scale" panel provides a scale based on the drawn line The "Scale" panel was used to resize the image in order to obtain a scale of 100 pixels/cm.*

6.3.1.2 Segmentation

In the "Segmentation editor" plugin (Schindelin *et al.*, 2007), we used the "Polygon selection" tool to draw each pad and add them (by clicking the "+" symbol) to a new window (Figure 9 A). Each track has five pads, identified as MP for Main Pad, T1 for Toe 1, T2 for Toe 2, T3 for Toe 3 and T4 for Toe 4. In this study, the direction of numeration of the toes was trigonometric.

Once the new windows contained the five components (Figure 9 B), we saved it as a *.jpg file named "Specimenxxx_all", where xxx is a specimen number given to each track. We then duplicated the image five times so that each component could be individually saved as *.jpg files. In each of the duplicated window, we selected four of the five components (using the "wand (tracing) tool") and deleted them, so that the remaining fifth could be saved and named "Specimenxxx_XX", where XX is the identification of the pad (Figure 10 A).

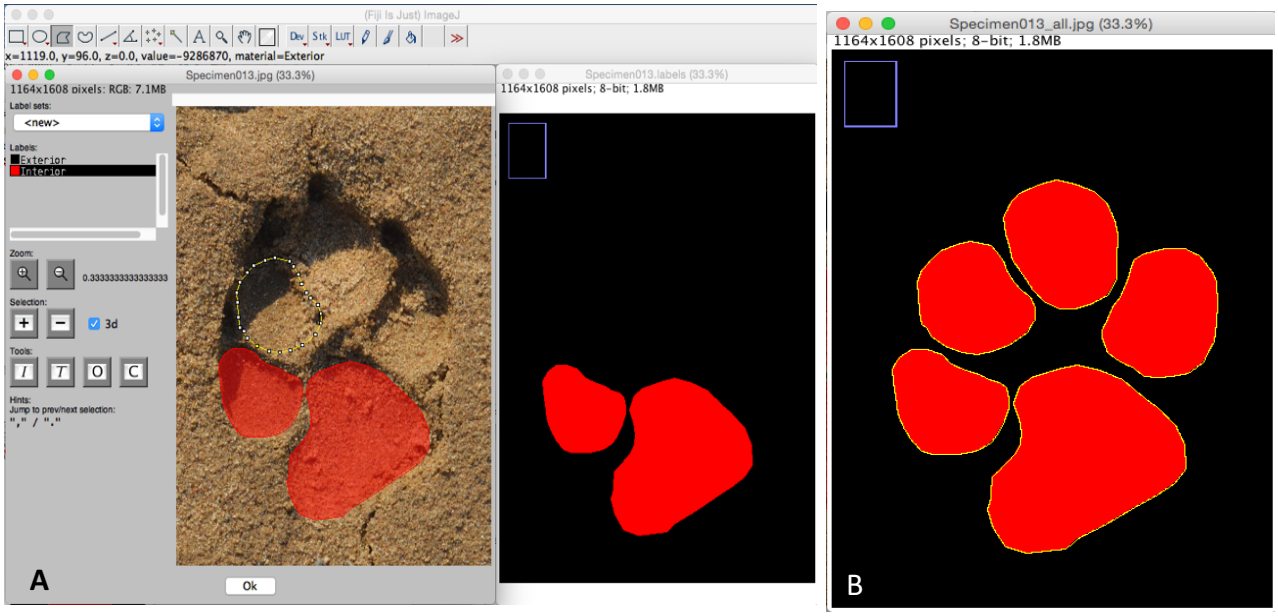

Figure 9 - *The segmentation of each pad conducted in the "Segmentation editor" plugin of Fiji (Schindelin et al., 2007). The "Polygonal selection" tool was used to draw the shape of each pad (in the left window of Figure 9 A), which is then added to the right window by clicking on the "+" button. Figure 9 B displays the image containing the entire segmented track, which is saved as "Specimenxxx_all.jpg".*

6.3.1.3 Fixed landmarks digitisation

Landmarks could have been digitized using the *digitize2d* function of the *Geomorph* package in R (see Section 6.4). However, a scaling error seemed to occur while importing the *.jpg image in *Geomorph* (see Section 6.4.1.1 and Appendix B for more details). We therefore positioned the fixed landmarks in Fiji using "Multi-point" tool (Figure 10 A). Their coordinates were then "saved as XY coordinates" in text files (hereafter *.txt), which we named "Specimenxxx_XX_fixed".

6.3.1.4 Curve extraction

To digitize semi-landmarks during geometric morphometric analyses (Section 6.4.1.2), the curve along the border of each pad had to be extracted from the rest of the model. To do so, we used the "Find edges" tool of Fiji (Figure 10 B), and saved the points that compose the curve as XY coordinates. We then named the new text files "Specimenxxx_XX_curve.txt".

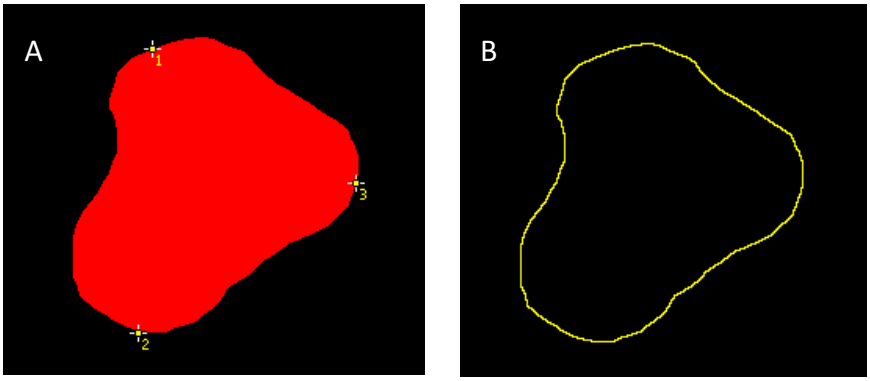

Figure 10 - *Digitisation of the fixed landmarks (A) and extraction of the curve (B) of the main pad of a track in Fiji.*

6.3.2 Three-dimensional (3D) models

6.3.2.1 3D-modelling in Photoscan

The 3D-modelling of tracks, using photogrammetry, was performed with Agisoft Photoscan Professional Edition version 1.2.6 build 2834 (Agisoft LLC, 2016) (hereafter PS). PS is a multi-view 3D reconstruction program that can create 3D content from at least two arbitrary images (Agisoft LLC, 2016). The 3D reconstruction comprises three main steps:

1) Photo alignment

The photo alignment step is divided into four sub-steps: (i) estimation of image quality, (ii) camera alignment, (iii) scaling, and (iv) optimization of the alignment.

Once the ten pictures of a track were added in the software, their quality was estimated by the "Estimate image quality" tool, which gives an index that ranges between 0 (low quality) and 1 (high quality). As recommended by Agisoft LLC (2016), we chose a threshold of 0.5 (i.e. we deleted all the images with a quality lower than 0.5). Additionally, we manually checked all the images in order to discard the blurred ones that may have been overlooked by the image quality index.

The "camera alignment" tool builds a sparse point cloud (Figure 11) by applying the "bundle adjustment" method. It consists of: (i) searching for the feature points (i.e. tie points) of each image and match them between photographs, (ii) finding the camera positions and orientations, and (iii) estimating the internal orientations (i.e. camera calibration parameters). For this step, we applied the parameters that were recommended by Marchal *et al.* (2016) (Appendix C).

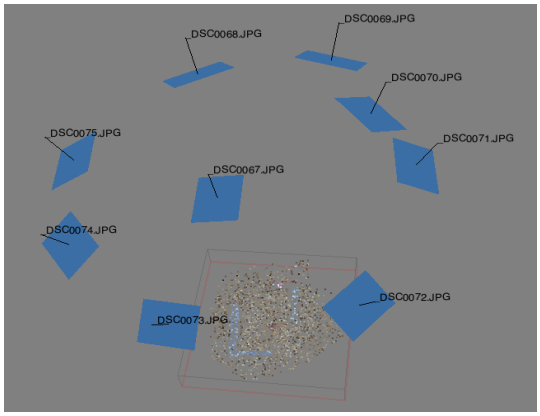

Figure 11 – *Visualisation of the sparse point cloud that results from the camera alignment process in Photoscan. Each blue square represents the position and orientation of one of the camera stations*

Once the alignment is completed, its quality and precision have to be verified. For each image, PS measures a re-projection error, which is defined as the "root mean square re-projection error calculated over all the feature points detected in the photograph" (Agisoft LLC, 2016). In other words, the re-projection error represents the distance between a projected point and the measured one (Gargallo et al., 2007). The "error (pix)" per image, which can be consulted in the "reference" tab, should not exceed the value of 0.8 (Agisoft help desk). Any image with an "error (pix)" higher than 0.8 was manually discarded.

In order to provide a scale to the model, we placed two markers twenty centimetres apart from each other on the graduations of a ruler, on one of the aligned photograph. To reduce the chance of misplacing them, *Photoscan* automatically projects predictor rays onto the remaining aligned photographs (Figure 12). Their locations can therefore be confirmed by re-positioning them on a second photograph. From those two markers, a scale bar can be created (in the "reference" tab), with a precision of 0.1mm (Agisoft LLC, 2016).

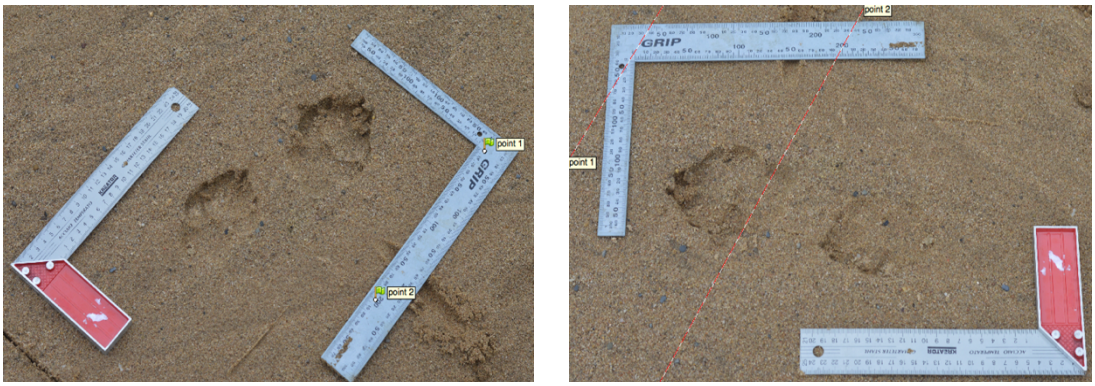

Figure 12 – *Positioning of markers on aligned photographs in Photoscan. Two markers are placed on a first image (A). Photoscan then projects predictor rays on a second image (B) to facilitate the placement.*

We finally applied an optimization step ("setting" and "optimize cameras" panels) using the parameters recommended by Marchal *et al.* (2016) (Appendix C), as it significantly reduces the re-projection errors of the aligned cameras (Marchal *et al.,* 2016).

2) Dense point cloud

To build a dense point cloud, PS applies a "Dense Multi-View 3D Reconstruction" (DMVR) algorithm, which operates on the pixel values of the aligned images (Verhoeven, 2011).

The quality of the dense point cloud has to be selected considering the following: the higher the quality, the denser the point cloud, the more faces the polygonal mesh will have. A "face" is a polygonal surface that is built between points that are in close proximity within the dense point cloud. Consequently, the denser the point cloud, the smoother the final mesh (see Step 3). Marchal et al. (2016) therefore recommended to apply the "ultra high" quality. However, in the present study, repetitive hardware failure during processing forced us to set the quality on "high" rather than "ultra high". Instead of having eight to nine million faces composing the mesh, the latter could only be made of two to three million faces. But considering that the morphometrics data depend on the position of the landmarks on the model and not on its smoothness, we assumed that this restriction would not have a significant effect on the final results of this study.

To deal with any potential outliers, *Photoscan* proposes three "depth filtering" intensities: mild, moderate, and aggressive. Because the software can sometimes identify small but important details of the model as outliers, we chose the "moderate" filtering option. Only the most significant outliers were therefore filtrated.

3) Mesh

Based on the points of the dense cloud, *Photoscan* finally builds a polygonal 3D-mesh that represents the surface of an object (in this case, a track). We selected the "high face count" option, which corresponds to the highest quality.

Among the other parameters (Appendix C), the selected surface type was "arbitrary", which allows the reconstruction of any type of object (in contrast with the option "height field", which concerns aerial photogrammetry) (Agisoft LLC, 2016).

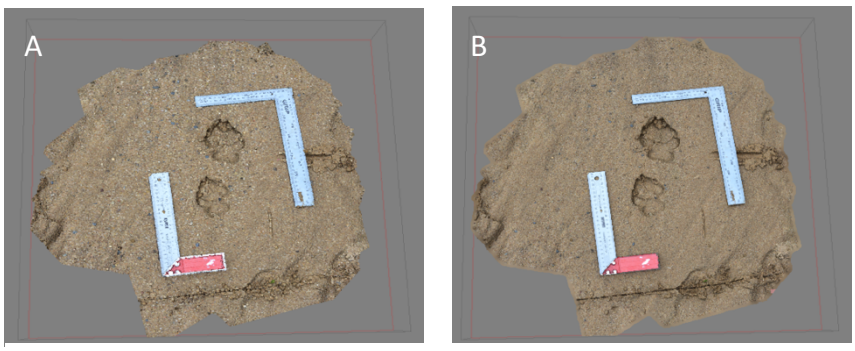

Figure 13 - *Dense point cloud (A) and 3D-mesh (B) of a track set.*

We then exported the mesh as a *.ply file so that we could import it in other software, such as *CloudCompare* for segmentation (Section 6.3.2.2) and R for statistical analyses with the *Geomorph* package (Section 6.4).

6.3.2.2 Segmentation in CloudCompare

As for 2D-images, the segmentation of the tracks using semi-automatic tools was not applicable due to the lack of contrast between each component of the track and the intact substrate. We therefore conducted the segmentation manually as well. However, in this case, the use of 3D-models reduces the human impact on the process (Marchal *et al.,* 2016): the tracks can be coloured according to their depth, making their contours more easily visible by the human eye.

The operations to add depth colours, performed by the software *CloudCompare* (version 2.8.1), can be divided into three steps:

1) Firstly, the depth of the track has to be aligned with the z-axis. To do so, we used the "Bounding box P.C.A. fit" tool, which aligns the tracks according to the principal components from the normal of the faces (Figure 14 B) (CloudCompare, 2015). We then separated each track from the rest of the mesh using the "rectangular selection tool" (Figure 14 C).

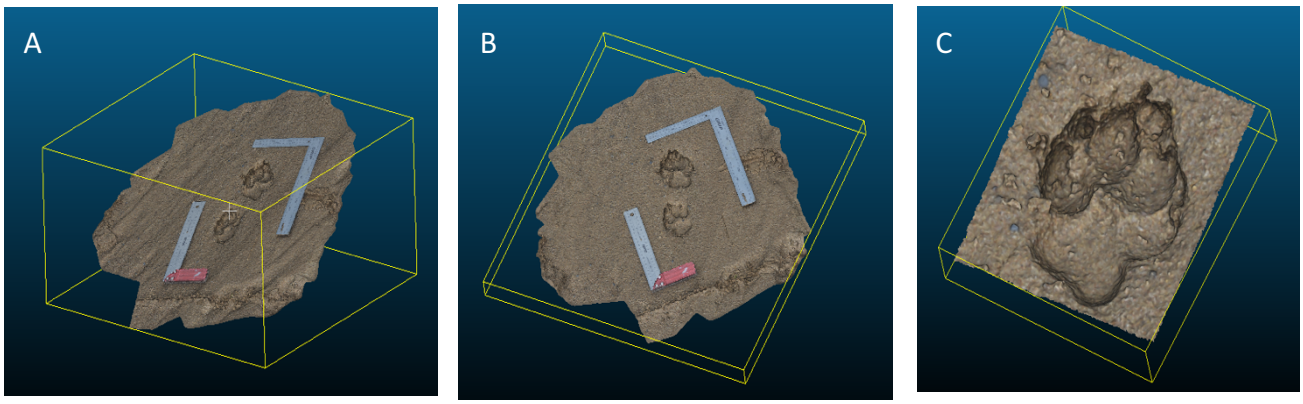

Figure 14 - *Alignment and first segmentation of a track in CloudCompare. Figure A represents the 3D-mesh once imported in CloudCompare; Figure B shows the mesh that has been aligned using the "P.C.A. Bounding Box" tool in order for the depth of the track to corresponds to the z-axis of the bounding box; Figure C displays a track that has been segmented from the rest of the mesh by using the "rectangular selection" tool.*

2) The "height ramp" tool then coloured the rectangular selection of the track according to its depth (i.e. the z-axis of the bounding box) by using the (Figure 15 A).

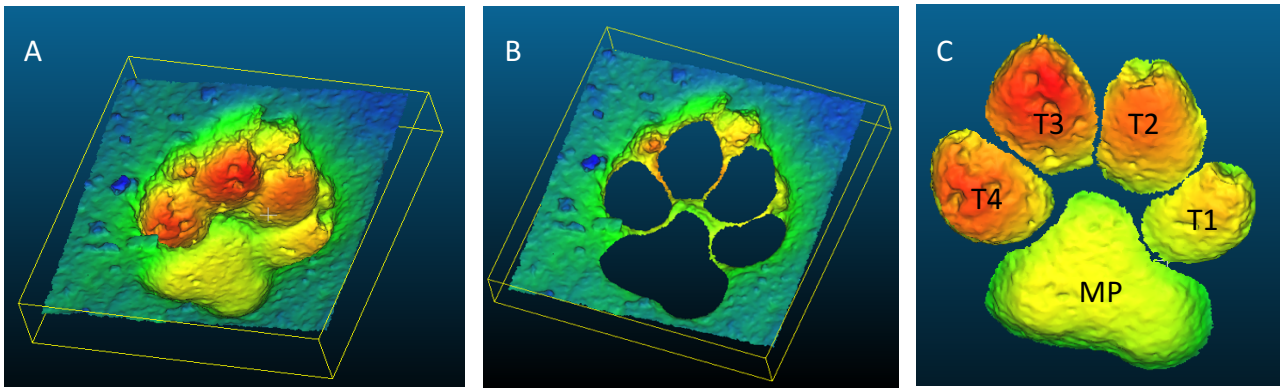

Figure 15 - *Segmentation of the different track components in CloudCompare. Once the track is coloured according to its depth (A), the mesh is manually segmented into the five components of the track (C) (MP for Main Pad, T1 to T4 for Toe 1 to Toe 4).*

3) The third step is the actual segmentation of the pads. As for 2D-images, we used the “polygonal selection” tool to extract the pads from the rest of the model. As mentioned earlier, a track has five pads, which are identified as the main pad (MP) or one of the four toes (T1 to T4). The latter were numbered trigonometrically (Figure 15 B). Once segmented, the mesh of each pad was saved as a *.ply ASCII file, and named “Specimenxxx_XX”, where xxx is a number given to each track (i.e. Specimen) and XX the identification of the pad.

A last step consisted of using the “merge” tool to regroup all the pads into one entire segmented track (Figure 16), which was then saved as a *.ply ASCII file named “Specimenxxx_all”. The additional information that can be extracted from it is the relative position of each pad (i.e. the distance between each pad).

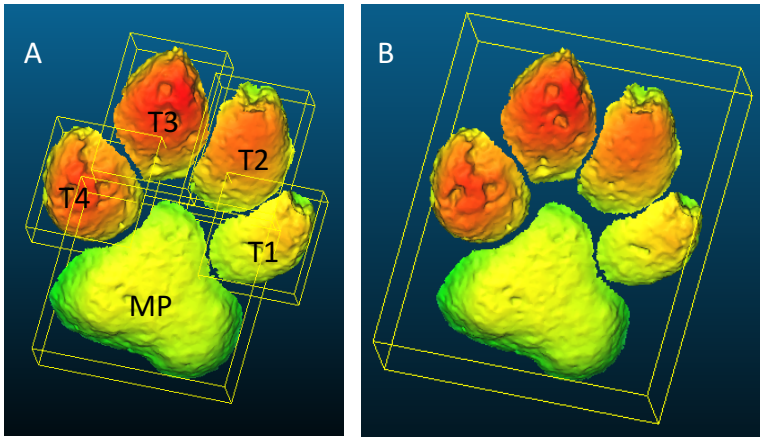

Figure 16 - *The mesh of each track component (A) and their regrouping into one entire segmented track (B) in CloudCompare.*

6.3.2.3 Extraction of a curve in Rhinoceros

To position semi-landmarks in *Geomorph* (see Section 6.4.1.2), the curves that represent the border of each pad had to be independently extracted. We used the software Rhinoceros (version 5.3.2) to extract the curve along the border of the mesh (“duplicate border” tool), transform it into points (“extract points” tool), which were then exported into *.txt files (“export selected” tool), under the same name as their pad of origin.

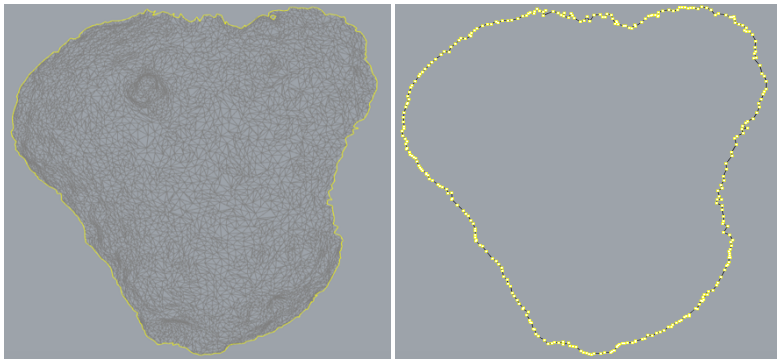

Figure 17 - *Curve extraction of a Main Pad in Rhinoceros. Figure A shows the mesh of the pad and its "duplicated border" (yellow line). Figure B shows the points extracted from the curve that corresponds to the border of the mesh.*

6.4 Geometric morphometrics in R

In the R statistical computing environment (R Development Core Team, 2017), *Geomorph* is a package used to perform shape analysis using geometric morphometrics (Adams *et al*., 2012). The main functions and their options are explained in details in the "Quick Guide to *Geomorph*" (Sherratt, 2015).

A preliminary step involves installing the different packages, other than *Geomorph* itself, that contain the functions that used throughout the analyses. For instance, the present study requires the packages *ggplot2*, *jpeg*, and *mass*. 2D- and 3D-models can then be imported using the functions "*read.jpeg*" and "*read.ply*" respectively. Once landmarks are digitized on the forms, *Geomorph* generates shape variables via Procrustes analyses, performs statistical analyses of shape variation and covariation, and provides graphical visualisations of shapes and patterns of shape variation (Adams *et al.,* 2013).

The statistical analyses described hereafter (Sections 6.4.2 to 6.4.4) were conducted on every possible "entity". In this study, we defined an entity as a combination of (i) a type of model (2D or 3D), the types of landmarks digitized on the pads (fixed, curve-sliders, and/or surface-sliders) and a type of object (Main Pad (MP), one of the four toes (T1 to T4), or the entire track). We initially analysed all the pads independently from each other, before regrouping them together as an entire "track" (Section 6.4.1.4) to analyse them as such.

Table 1 - *The different entities on which the Procrustes analyses were conducted. An entity is a combination of (i) a type of model (2D or 3D), the types of landmarks (fixed, fixed and curve-sliders, or fixed and curve- and surface-sliders) and a type of object (Main Pad (MP), one of the four toes (T1 to T4) or the entire track (track)).*

Type of model	Type of landmarks	Pads					Track
		MP	T1	T2	T3	T4	
2D	Fixed	Entity 1	Entity 2	Entity 3	Entity 4	Entity 5	Entity 26
	Fixed+curve	Entity 6	Entity 7	Entity 8	Entity 9	Entity 10	Entity 27
3D	Fixed	Entity 11	Entity 12	Entity 13	Entity 14	Entity 15	Entity 28
	Fixed+cure	Entity 16	Entity 17	Entity 18	Entity 19	Entity 20	Entity 29
	Fixed+curve+surf	Entity 21	Entity 22	Entity 23	Entity 24	Entity 25	Entity 30

6.4.1 Digitisation of landmarks

The functions used to digitize landmarks depend on the type of landmarks and the type of model (Sherratt, 2015). In this study, we used three types of landmarks: (i) fixed landmarks, which would be accepted in Bookstein's "Type 1" and "Type 2" categories (Section 3.2.2), (ii) curve-sliders and (ii) surface-sliders, which are semi-landmarks that can slide along the structure to which they belong (a curve or a surface respectively).

6.4.1.1 Fixed landmarks

Fixed landmarks can be interactively digitized on the 2D and 3D models using the functions "*digitize2d*" and "*digit.fixed*" respectively. In both cases, the number of landmarks has to be mentioned in the function.

With the function "*digitize2d*", we can process a list of *.jpg files sequentially. The output is one single *tps file that contains every landmark coordinates of all the specimens. However, due to a scaling error that consistently led to a displacement between the coordinates of fixed landmarks and the ones of the curve-sliders (Appendix B), we digitized the 2D-fixed landmarks in Fiji (Section 6.3.1.3). After importing the *.txt files in *Geomorph*, we grouped all the coordinates together in a 3D-matrix. This matrix, called an array (Appendix D), is the standard format on which most *Geomorph* analysis functions can be conducted (Appendix D) (Sherratt, 2015).

The function "*digit.fixed*" digitizes 3D-landmarks on one specimen at a time, resulting in one *.nts file for each. Once all the 3D-landmarks are created, the function "*readmulti.nts*" groups all the *nts files into a single 3D-matrix.

In this study, we digitized three fixed landmarks on the main pad: one in the middle of its highest curve, and two in the middle of the two lower left and right curves. Four fixed landmarks characterized each toe: two at the extremities of the longest axis of the ellipse-shaped toe, and two others were in the middle of the side curves (Figure 18 A).

6.4.1.2 Semi-landmarks on curve

The digitisation of curve-sliders on a specimen is based on the curve that was extracted during image processing (Sections 6.3.1.4 (2D) and 6.3.2.3 (3D)). Once the *.txt file containing the point coordinates of a curve is imported, the function "*digit.curve*" selects a given number of points that are evenly spread along the curve. Those points are initially registered as fixed landmarks, so they need to be defined as sliders afterwards. To do so, the manipulator can either use the function "*define.slider*", or import a matrix identifying them (Sherratt, 2015).

In this study, we used fifty curve-sliders to characterize the main pad, and twenty for each toe. We added their coordinates to the ones of the fixed landmarks, so that we could conduct the Generalized Procrustes Analyses (GPA) on 53 landmarks (i.e. 3 fixed and 50 curve-sliders) for the main pad, and 24 (i.e. 4 fixed and 20 curve-sliders) for each toe (Figure 18 B).

6.4.1.3 Semi-landmarks on surface

Sliders were also used to characterize the surface of the 3D-meshes. The function "*buildtemplate*" digitizes a given number of landmarks on a single specimen, which has to be representative of the consensus configuration. The function "digitsurface" then digitizes homologous landmarks on the other specimens based on that template. As for the curve-sliders, the newly-digitized landmarks need to be defined as surface-sliders by importing a matrix identifying them.

Fifty surface-sliders were digitized on the main pads and twenty on each toe. We then added them to the matrix that already contained the fixed landmarks and curve-sliders, and conducted the GPA on the 103 (i.e. 3+50+50) landmarks of the main pad and the 44 (i.e. 4+20+20) landmarks of each toe (Figure 18 C).

6.4.1.4 Entire track

To take into consideration the relative position of the track components to each other, the landmarks of each pad were grouped together in a single "entire track" model. To do so, we successively added the landmarks of the toes to the matrix of the main pad. The resulting entire track (i.e. "Specimenxxx_all"), was therefore characterized by 19 landmarks in the "fixed" only entity, 149 landmarks in the "fixed+curve", and 279 in the "fixed+curve+surface" (Figure 18).

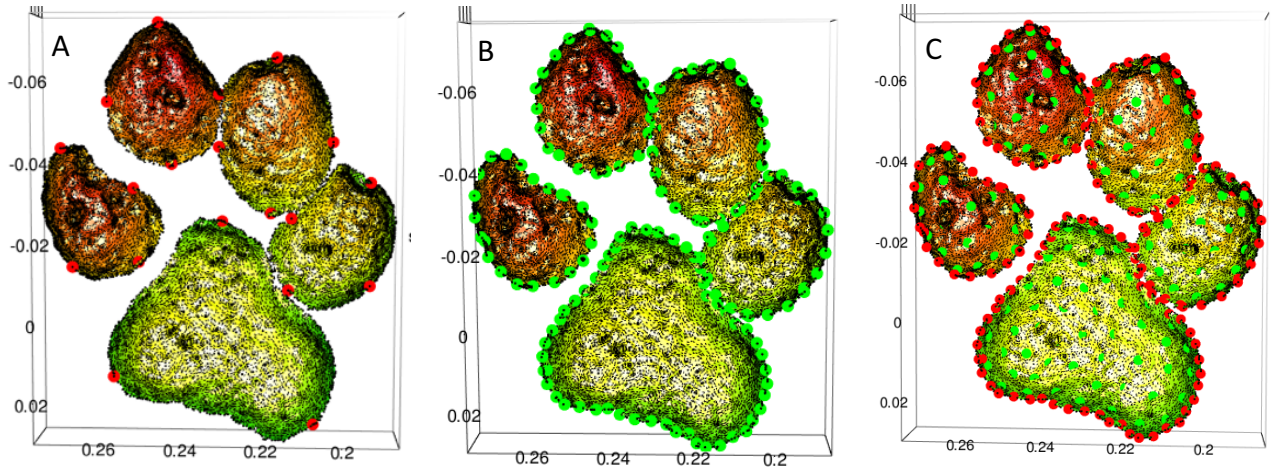

Figure 18 – *Location of fixed landmarks (A), fixed landmarks and curve-sliders (B), fixed landmarks, curve-sliders and surface-sliders (C) on the entire track of a specimen.*

6.4.2 Generalized Procrustes Analysis (GPA)

Once the landmark coordinates of all the specimens are grouped into a 3D-matrix, the function "*gpagen"* runs a GPA that calculates the coordinates of the landmarks of the mean shape, as well as the Procrustes coordinates and centroid size of each specimen. Note that if semi-landmarks on curves or on surface are included, matrices defining them must be specified beforehand and referred to within the function (Sherratt, 2015).

We used the function "*plotAllSpecimens*" to visualize the superimposed models (Figure 19). To connect the landmarks of the mean shape, a matrix of links can be imported and read by the function (Sherratt, 2015).

To verify that no landmark was misplaced by the manipulator, we used the function "*plotOutliers*" to "create a plot of all the Procrustes-aligned specimens ordered by their distance from the mean shape" (Sherratt, 2015). The specimens falling outside the upper quartile range (coloured in red in the plot) were potential outliers (Figure 20 A). To check that they were not due to an inversion

between landmarks (in which case, the landmarks of that specimen have to be re-digitized), we inspected them individually using the function "*plotRefToTarget*". This function plots the mean shape of the aligned specimens and the shape of the potential outlier (Figures 20 B and C).

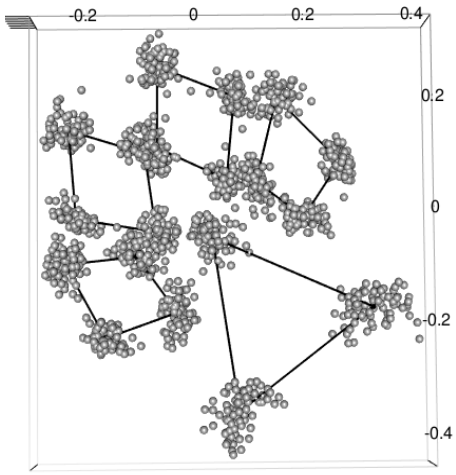

Figure 19 – *The mean configuration of the entire tracks, drawn by the function "plotAllSpecimens" in Geomorph. The grey dots correspond to the Procrustes coordinates of each specimen. The black lines connect the landmarks whose coordinates are the average of the Procrustes coordinates.*

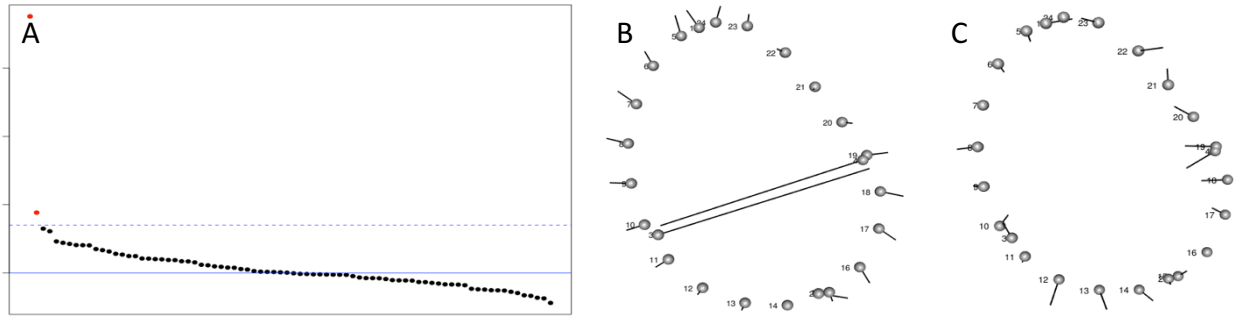

Figure 20 - *Verification of potential outliers after the superimposition. Figure A displays the graph resulting from the "plotOutliers" function. Specimens falling above the upper quartile (dashed line) are plotted in red and need to be inspected. Figures B and C are the outputs of the function "plotRefToTarget". They display the mean shape of the aligned specimen (grey dots) and the shape of the potential outlier (whose landmarks are located at the other end of the black line). Figure B corresponds to the specimen whose dot is the highest in the "plotOutliers" graph. The two lines that cross each other indicates that there has been an inversion between those two landmarks. Figure C corresponds to the specimen whose dot lands just on top of the upper quartile. No line crosses each other, which implies there has been no landmark inversion: the specimen is a small outlier that can still be taken into account for the next analyses.*

6.4.3 Shape and Csize Analysis

During the Procrustes superimposition the information on the size of each specimen is separated from the information on their shape, and indexed as their centroid size (Sections 3.2.1 and 3.2.3). We could therefore estimate the influence of track position on each type of variable (shape and size) independently from on another.

An analysis of variance (ANOVA) has two purposes: (i) to test the hypothesis that the means of the compared populations are equal, and (ii) to assess the importance of one or more factors by comparing the response variable means at the different factor levels (Minitab Inc, 2017).

6.4.3.1 Procrustes ANOVA

In geometric morphometrics, the Procrustes ANOVA, which is performed by the function "*procD.lm*" on the Procrustes coordinates, has been designed specifically for the analyses of shape data. It avoids the problems that are due to (i) the matrices from GPA-aligned coordinates that are singular, and (ii) the datasets that often have more variables than specimens. The function "quantifies the relative amount of shape variation that is attributable to one or more factor in a linear model" (Sherratt, 2015). In this case, it tests if the factor "track position" has a significant effect on the shape of the track. The level of significance is $p \leq 0.05$.

6.4.3.2 Centroid size

To conduct an ANOVA on the distribution of a variable, the normality of the distribution and the equality of variances first have to be verified. We conducted *Shapiro-Wilk tests* to test the normality and *Bartlett's test* for the equality of variances (The R Stats Package, 2017). In both cases, a p-value higher than 0.05 validates their null hypotheses, i.e. the distribution is normal and the variances of each population are equalled. If both conditions were met, we conducted an ANOVA. A p-value lower than 0.05 indicated that the influence of track position on the size was significant (i.e. the centroid sizes of each track position were significantly different). A *TukeyHSD* test (Tukey Honest Significant Differences) was then conducted to analyse which of the track position had a centroid size significantly different from the others (The R Stats Package, 2017).

If one of the conditions for the ANOVA was not met (normality or equality of variances), we conducted a *Kruskal-Wallis Rank Sum Test*. As for the ANOVA, a p-value that was lower than 0.05 indicated that track position had a significant influence on the size of a track.

6.4.4 Principal Components Analysis (PCA)

"A Principal Component Analysis (PCA) is a statistical procedure used for identifying a smaller number of uncorrelated variables, called 'principal components', from a large set of data. Its goal is to explain the maximum amount of variance with the fewest number of principal components" (Minitab Inc, 2017). In other words, a PCA decreases the dimensionality of the dataset.

A characteristic of the principal components (hereafter, PC) is that the sum of their variance equals the total variance of the dataset. The contribution of each PC can therefore be expressed as an Eigen value, also called "score". The main variability of a dataset can usually be explained by only a few PC. The choice of the number of PC to be kept for further analyses is a compromise between the number of PCs and the amount of information they bring all together (i.e. their cumulative proportion of variance): the quality of the analysis is proportional to the percentage of the variance that is explained, but the more PC, the harder the interpretation. For instance, the proportion of variance explained by two PC can be represented in a graph such as the one shown in Figure 21: each specimen is represented by a unique point whose coordinates correspond to its PC scores along the PC1 and PC2 axes. Also, each point can be coloured according to the group factor (in this case, the track position) that its specimen belongs to. This enables us to estimate the discrimination power of those two PC, i.e. if their cumulative proportion of explained variance is enough to discriminate the different track position.

In *Geomorph*, the function "*plotTagentSpace*" performs PCA. The package *ggplot2* contains the function used to plot graphs such as the one in Figure 21. Additionally, we drew thin-plate spline deformation grids (using the function "*plotRefToTarget*") to represent the shape at the extremes of the range of variability along the two axes (i.e. to visualize the deformation of the shape between the mean configuration and the configuration of the specimens that range the furthest away from it according to PC1 and PC2).

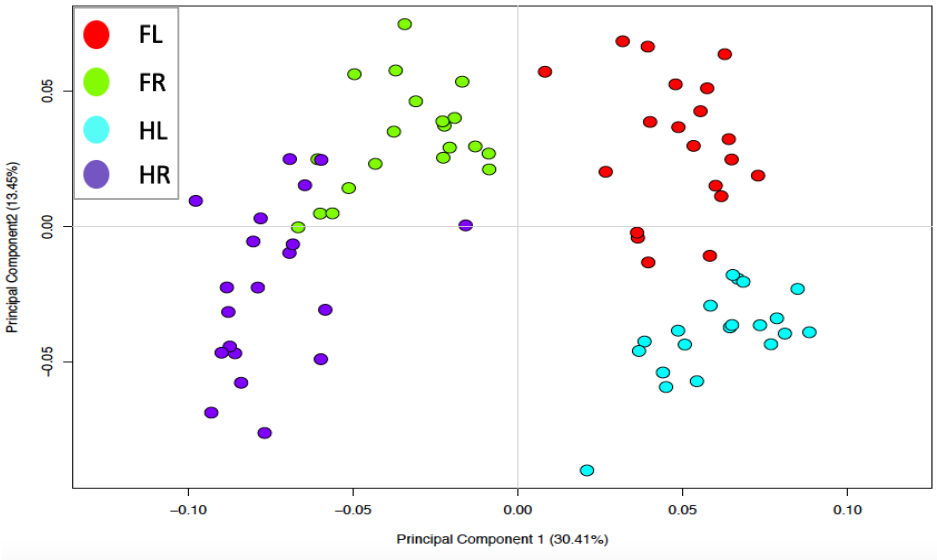

Figure 21 - *Principal Component Analysis applied on the Procrustes coordinates of an entire track. The scores of the two principal components range along the two axes. Each specimen is represented by a dot whose coordinates therefore correspond to the PC scores of the specimen for the two first PCs. The colour code represents the position of each track: red for Front Left (FL), green for Front Right (FR), blue for Hind Left (HL), and purple for Hind Right (HR).*

6.4.5 Linear Discriminant Analysis (LDA)

Linear Discriminant Analysis (LDA) is a classification method that searches for a linear combination of variables that best separates two or more classes (Sayad Saed, 2017). It creates an algorithm which, by taking into consideration a certain number of variables (i.e. the principal components originating from the PCA), is able to determine in which class (in this case, one of the track position) a specimen belongs to. In R, the package *mass* (Venables et al., 2002) contains the function "*lda*", which creates discriminant functions on centred variables.

The quality of a LDA is given by the accuracy of prediction of its algorithm. This accuracy can be calculated using two different manners: with or without "Jack-knife". The standard LDA ("without Jack-knife") uses all the observations both for the calibration of the LDA model and for the estimation of the error rate. It is therefore less likely that the model places a track in a wrong class. The LDA with "Jack-knife", on the other hand, builds the model with all the observations except one, which is used afterwards to test the model. The process is repeated for every observation, using a different one to test the model every time. The "jack-knife error" is then calculated as the number of models that assigned a wrong class to a specimen divided by the total number of models tested.

The aim of this study is to provide future wildlife research with an algorithm that is able to identify unknown sampled tracks, i.e. tracks that have not been used for the calibration of the LDA model. We therefore chose to apply LDA with Jack-knife, as it better corresponds to the future use of the algorithm

LDA were conducted on different scenarios. We defined a scenario as a combination of (i) a recording technique (2D or 3D), (ii) a feature extraction method (traditional or geometric approaches, with fixed landmarks, curve- or surface-sliders), (iii) a type of object (independent pads or entire track), and (iv) a type of variable (shape, size, or both shape and size).

Note the difference between the two types of object: a LDA applied on the "independent pads" takes into consideration the PC scores that each pad obtained independently from each other (entities 1 to 25 defined in Table 1, Section 6.4). A LDA applied on the "entire track" takes into consideration the results of the PCA that was directly conducted on the entities 26 to 30 (Table 1). To simplify the description of the results, the entities that concern the independent pads and the entire tracks were refered to as "pad" and "track" respectively.

The types of variables refer to which information resulting from the Procrustes superimposition (size and/or shape) is used by the LDA. To estimate which type of variables has the most impact on the identification of the track position, we applied LDA (i) on the shape components only ("shape"), (i) on the centroid size only ("Csize"), and (iii) on both at the same time ("Shape&Csize").

For each scenario, we applied several LDA using an increasing number of variable (i.e. PC). We then selected the algorithm with the highest accuracy of prediction within a scenario, and used it as a criterion to determine which scenario could procure the most accurate algorithm. The relation between the accuracy of an algorithm and the number of variables that it took into account was

studied as well. By comparing the trend curves of each scenario, other comparative approaches could be used. For instance, instead of selecting a scenario by only considering the maximum accuracy obtained by one of its algorithms, scientists could either (i) set a maximum number of PC in order to limit its complexity, or (ii) set a minimum accuracy which would be considered as acceptable for their study. In the first case, the algorithm that obtained the highest accuracy with less PC than the maximum set would be selected; in the second case, it is the algorithm that reaches the set accuracy with the minimum number of PC that would be selected.

6.5 Traditional morphometrics in R

Because the data extracted through geometric morphometrics consists of x-y-(z-)coordinates of landmarks, the distances between each pair of landmarks can be reconstructed from these coordinates. In other words, all the information that is extracted using traditional morphometric (in this case, distances between landmarks) can be obtained from the information extracted through geometric morphometric (which is the coordinates of these same landmarks).

Once the files containing the fixed landmark coordinates were grouped together into a 3D matrix, the Euclidian distances were simply measured by the function "*dist*" (The R Stats Package, 2017). There were 29 distances for the "pads" scenario (Figure 22 A) and 351 for the "track".

As for geometric morphometrics, we applied a PCA to decrease the dimensionality of the data sets, and ran several LDA by using increasing number of PC (both for the independent pads and entire tracks).

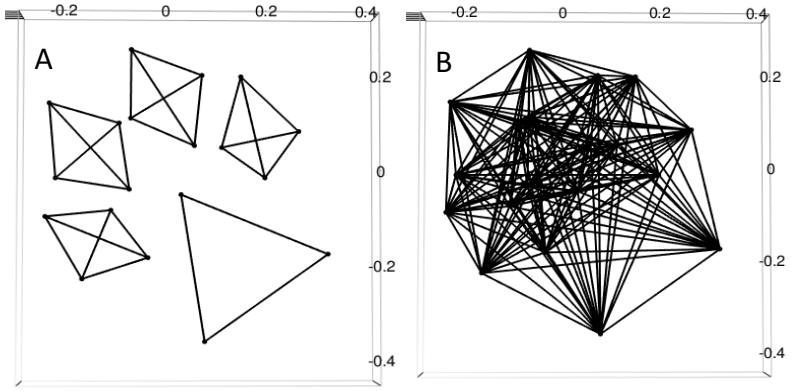

Figure 22 – *Schematics of the Euclidean distances extracted from the "pads" (A) and "track" (B) entities using traditional morphometrics analyses. Each line represents one of the distances measured by the "dist" function in R*

7 RESULTS

The entity “2D – fixed+curve” of the Toes 2, 3 and 4 could not be analysed, as a displacement between the coordinates of the fixed landmarks and the ones of the curve-sliders kept occurring (see Appendix B for more details on the matter). As this issue could not be solved at the time, we could not conduct LDA on scenario “2D – fixed+curve – pads”. However, although the same *.txt files (with the same coordinates) were used for the “2D – fixed+curve – track” scenario, such displacements were not observed, so the LDA analyses could be conducted normally.

7.1 Dataset

A total of 224 track sets of spotted hyena (i.e. 448 tracks) were sampled in Hluhluwe-iMfolozi Park, all in sandy soil along riverbeds. Considering the time necessary for image processing (both in 2D and 3D), twenty tracks from each position (i.e. 80 tracks in total) were randomly selected from the database.

If several pictures of a track presented alignment errors that were too high (see Section 6.3.2.1), or if the quality of the track was really too low (i.e. the contours of the pads not distinguishable at all), the track was discarded (both in 2D and 3D) and another one, from the same position, was randomly selected from the database to replace it.

7.2 Consensus configuration and centroid size

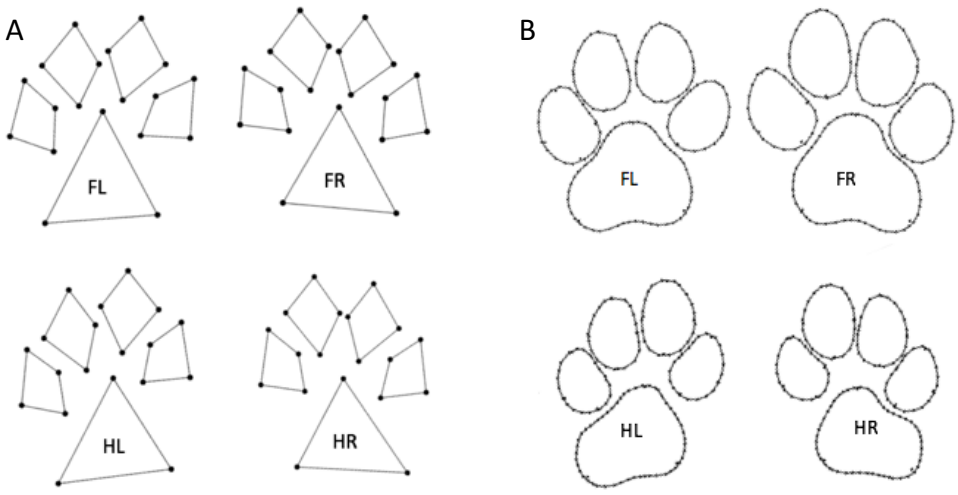

Figure 23 – *Mean configurations of track positions, represented by fixed landmarks only (A) and fixed landmarks and curve-sliders (B) on entire tracks. “FL” = Front Left; “FR” = Front Right, “HL” = Hind Left and “HR” = Hind Right.*

In geometric morphometrics, the Procrustes superimposition separates the size variable from the shape variables. The influence of track position could then be tested on the two types of variables independently from one another. The complete results of all the statistical tests involved in these analyses can be consulted in Appendix E. Tables 2 and 3 hereafter present the p-values that determined the level of significance of the influence of track position.

7.2.1 Influence of track position on shape

A Procrustes ANOVA was conducted on each entity (Table 2; Appendix E).

The influence of track position on the shape of the main pad and of the entire track was always highly significant (p=0.001). When both fixed landmarks and curve-sliders were used ("fixed+curve"), the influence was significant for all types of objects (i.e. pads or track) and both types of models (i.e. 2D or 3D), with the exception of Toes 2, 3 and 4 (T2 to T4) in 2D, for which we could not do the analyses. When only fixed landmarks ("fixed") or the three types of landmarks ("fixed+curve+surface") were considered, the level of significance of the influence of the track position varied from one toe to another with no particular pattern.

Table 2 – *Influence of track position on the shape of each pad and entire track. The Procrustes ANOVAs provide a p-value for each entity (defined in table 1, chapter 6.4), which indicates the level of significance of the influence. The influence is significant when p<0.05. "MP" stands for Main Pad, "T1" for Toe 1, "T2" for Toe 2, "T3" for Toe 3, and "T4" for Toe 4. "Track" corresponds to the entity that takes into consideration the "entire track". The complete results of the Procrustes ANOVA can be consulted in Appendix E.*

Type of model	Type of landmarks	Pads					Track
		MP	T1	T2	T3	T4	
2D	Fixed	0.001	0.005	0.001	0.001	0.069	0.001
	Fixed+curve	0.001	0.006	NA	NA	NA	0.001
3D	Fixed	0.001	0.067	0.650	0.006	0.051	0.001
	Fixed+curve	0.001	0.001	0.021	0.005	0.001	0.001
	Fixed+curve+surface	0.001	0.001	0.056	0.036	0.032	0.001

7.2.2 Influence of track position on size

The size distributions of 2D entities were all normal (p>0.005 for all Shapiro-Wilk tests), except for "2D – fixed – T3", and the variances were equalled (p>0.05 for all Bartlett's tests). On the other hand, the centroid sizes of 3D entities met the condition concerning the equality of variances, but none of normality.

The ANOVA that were conducted on 2D entities, as well as the Kruskal test on "2D – fixed – T3", indicated that the track position had a significant influence on the centroid size (Table 3). The *TukeyHSD* function revealed that the significant differences occurred only between a front track and a hind track (p<0.001), whereas the centroid sizes of the two front tracks (or the two hind tracks)

were not significantly different from each other (p>0.900) (Appendix F). The centroid sizes of 3D entities, on the other hand, were never influenced by track position. This was confirmed by simply visualizing their distributions as boxplots, such as the example in Figure 24.

Table 3 – *Influence of track position on the centroid size of each pad and entire track. ANOVA were conducted on the entities that presented normal distributions (all the 2D entities, except "2D – fixed – T3"); Kruskal-Wallis Rank Sum Test were conducted on entities whose distribution were not normal (all the 3D entities, as well as "2D – fixed – T3"). Both types of analyses provide a p-value which indicates the level of significance of the influence. The influence is significant when p<0.05. "MP" stands for Main Pad, "T1" for Toe 1, "T2" for Toe 2, "T3" for Toe 3, and "T4" for Toe 4. "Track" corresponds to the entity that takes into consideration the "entire track". The complete results of the analyses are presented in Appendix F.*

Type of model	Type of landmarks	Pads					Track
		MP	T1	T2	T3	T4	
2D	Fixed	< 0.001	< 0.001	< 0.001	< 0.001	< 0.001	< 0.001
	Fixed+curve	< 0.001	< 0.001	NA	NA	NA	< 0.001
3D	Fixed	0.497	0.460	0.548	0.605	0.561	0.645
	Fixed+curve	0.530	0.443	0.513	0.612	0.573	0.748
	Fixed+curve+surface	0.533	0.417	0.495	0.618	0.533	0.710

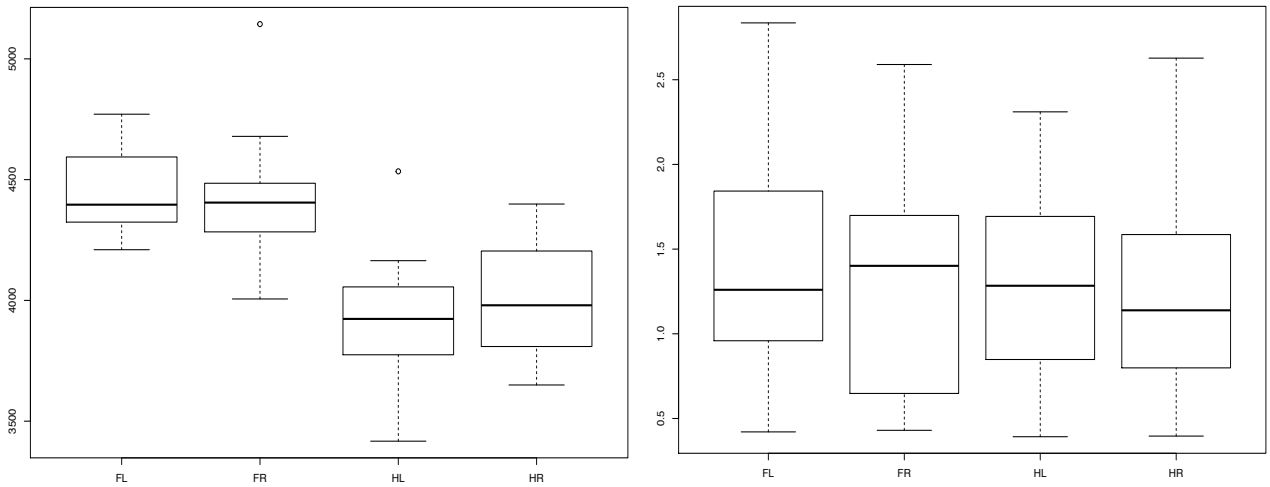

Figure 24 – *Boxplots of the centroid sizes of the entities "2D – fixed+curve –track" (A) and "3D – fixed+curve –track" (B). The x-axis refers to the position of the tracks: "FL" for Front Left, "FR" for Front Right, "HL" for Hind Left and "HR" for Hind Right. The y-axis gives the values of the centroid sizes; the bold horizontal line corresponds to the median of the distribution; the boxes represent the interquartile range (i.e. encloses 50% of the specimens); the dashed lines give the total range of the distribution except for "outliers".*

7.3 Principal Component Analyses

In geometric morphometrics, a principal Component Analyses (PCA) was conducted on ever possible entity (except T2 to T4 in 2D), each corresponds to a combination of (i) a type of model, (ii) a type of landmarks, and a type of object (one of the pad or the entire track).

The cumulative proportion of variability explained by the two first components (Table 4) was higher for the "2D – fixed –Toes" (T1 to T4) than the one for the "3D – fixed – Toes" (60 to 70% for the first versus 50 to 60% for the second). However, the PCA plots of most "pads" entities (both in 2D and 3D) showed that their two principal components were not sufficient to discriminate the different track positions (Figure 25). Some of the "MP" (Main Pad) entities could approximately discriminate the right and left tracks, but not the front and hind (Figure 25).

Table 4 – *Cumulative proportion (in %) of variability explained by the two first components (PC1 and PC2), and number of PC (in brackets) necessary to attain a cumulative proportion of 90%.*

Type of model	Type of landmarks	Pads					Track
		MP	T1	T2	T3	T4	
2D	Fixed	100.00 (2)	67.52 (3)	66.50 (4)	67.78 (4)	70.18 (4)	42.61 (13)
	Fixed+curve	70.00 (7)	53.15 (8)	NA	NA	NA	44.85 (19)
3D	Fixed	100.00 (2)	59.96 (4)	56.82 (5)	60.89 (4)	54.61 (4)	45.79 (17)
	Fixed+curve	61.95 (17)	29.21 (19)	29.40 (21)	30.16 (21)	33.65 (19)	43.86 (34)
	Fixed+curve+surface	51.45 (25)	26.01 (25)	30.36 (26)	34.30 (25)	38.92 (24)	40.20 (41)

On the other hand, the two first PC of the "track" entities explained 40 to 46% of its shape variability. These cumulative proportions were always lower than both "2D – fixed – pads" and "3D – fixed – pads", but higher than "3D – fixed+curve – Toes" and "3D – fixed+curve+surface – Toes"

In spite of their relatively low proportions of explained variance, the PCA plots of the "track" entities always discriminated the different track positions more efficiently than any "pads" entities. For every "pads", the two first PC were not able to separate the different track positions (Figure 25). However, for every "track" entity on which we conducted geometric morphometrics, PC1 always discriminated right from left while PC2 discriminated front from hind (Figure 26). However, the front/hind separation was not as strong as the right/left one, especially for the "2D – track" entities. Also, the PCA that were conducted on "fixed+curve" entities showed a stronger discrimination power than the ones conducted on "fixed" only entities (Figure 26), while the "fixed+curve" and "fixed+curve+surface" in 3D did not seem to be significantly different.

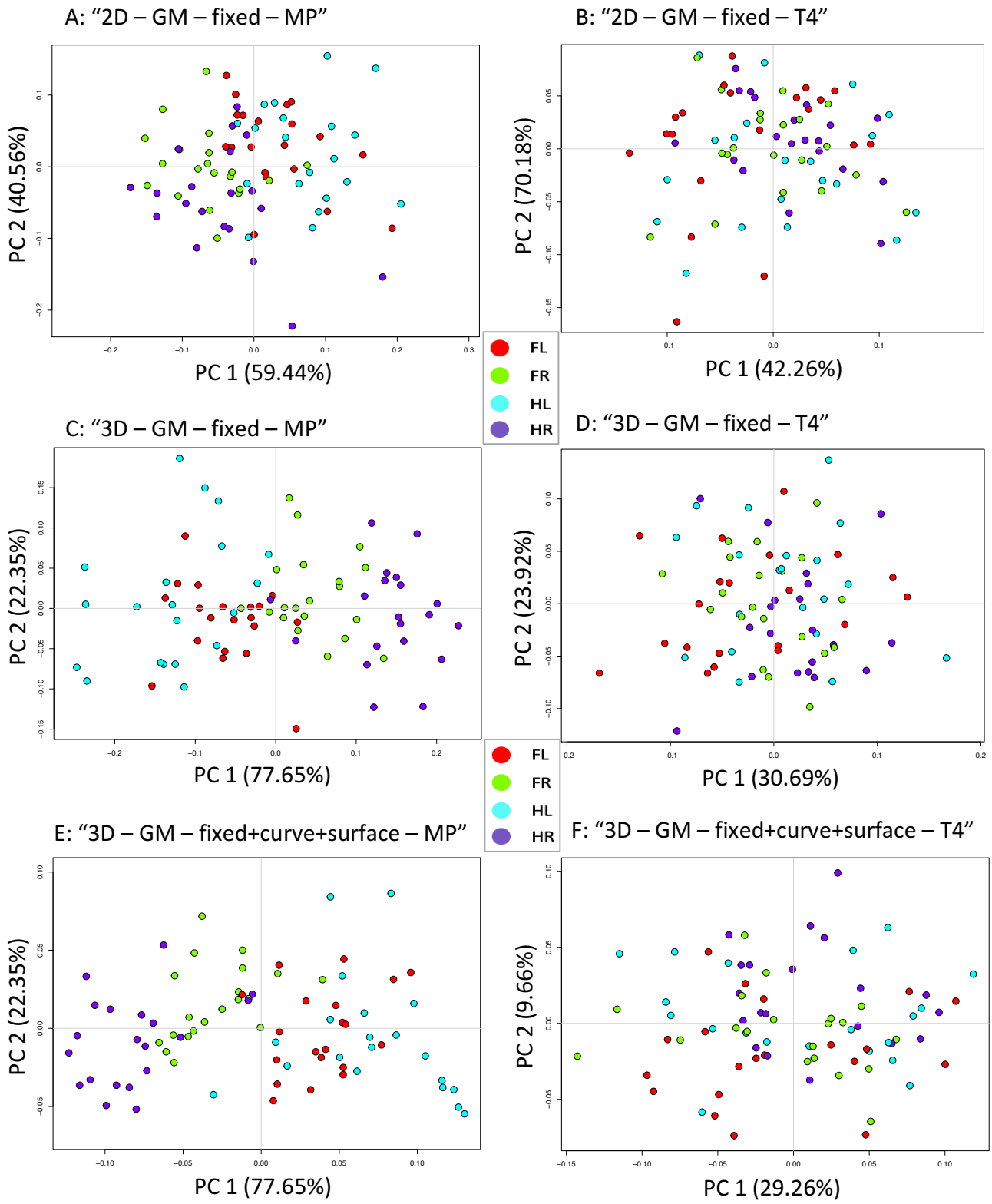

Figure 25 – *PCA plots resulting from Principal Component Analyses conducted on " pads" entities. Each PCA plots (A to F) corresponds to one entity: "GM" = Geometric Morphometrics; "fixed" = only fixed landmarks were used; "fixed+curve+surface" = the three types of landmarks were used (fixed, curve- and surface-sliders); "MP" = Main Pad; "T4" = Toe 4. The PCA plots of all the other entities can be consulted in Appendix G. The colour code represents the track position: red for Front Left (FL), green for Front Right (FR), blue for Hind Left (HL) and purple for Hind Right (HR).*

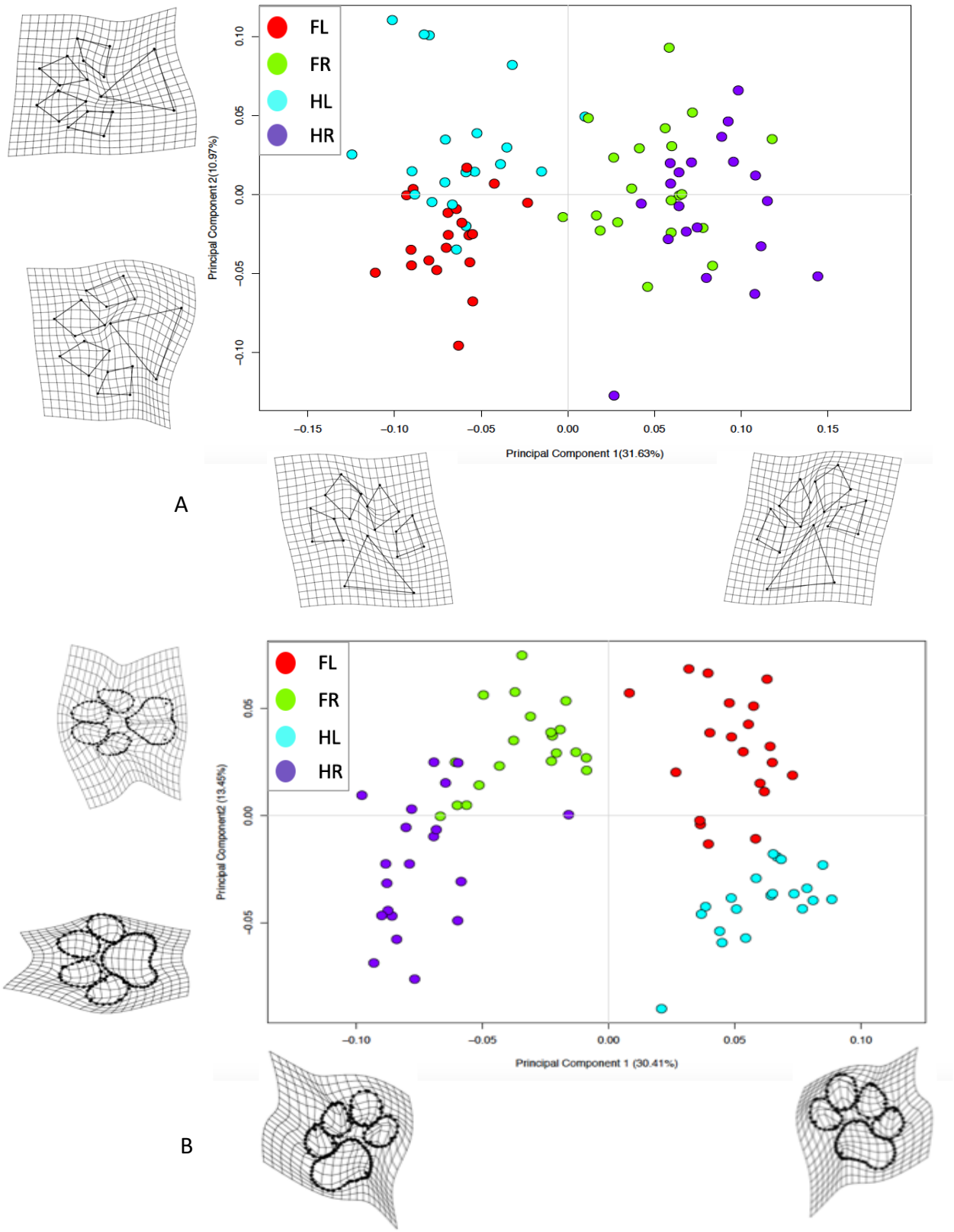

Figure 26 - PCA plots resulting from Principal Component Analyses conducted on the entities *"2D – fixed – entire track" (A) and "3D – fixed+curve – entire track" (B). The thin-plate spline deformation grids show the shape difference between the extremes of each principal component axis and the mean shape.* The PCA plots of all the other entities can be consulted in Appendix G. *The colour code indicates the position of the tracks: red for Front Left ("FL"), green for Front Right ("FR"), blue for Hind Left ("HL"), and purpled for Hind Right ("HR").*

7.4 Linear Discriminant Analyses

For each possible scenario, we conducted several Linear Discriminant Analysis, each with an increasing number of principal components (PC) originating from the PCA. All the accuracies of prediction can be consulted in Appendix H. The algorithm with the highest accuracy within each scenario was selected and used as a first criterion to compare the different scenarios (Table 5).

Table 5 - *The maximum accuracy of prediction of an algorithm resulting from the LDA of each possible scenario, and the number of principal components (PC) necessary to attain that accuracy. "TM" and "GM" stand for Traditional and Geometric Morphometrics respectively.*

Scenarios				Maximum accuracy (%)	Number of PC
Type of model	Feature extraction – Type of landmarks	Type of object	Type of variable		
2D	TM – fixed	Track	Distances	97.5	8
		Pads	Distances	82.5	20
	GM – fixed	Track	Csize	50.0	1
			Shape	87.5	7
			Shape&Csize	98.8	15
		Pads	Csize	56.3	1
			Shape	56.3	38
			Shape&Csize	80.0	28
	GM – fixed+curve	Track	Csize	26.3	1
			Shape	96.3	10
			Shape&Csize	98.8	10
3D	TM – fixed	Track	Distances	91.3	23
		Pads	Distances	57.5	5
	GM – fixed	Track	Csize	26.3	1
			Shape	97.5	11
			Shape&Csize	97.5	11
		Pads	Csize	38.9	1
			Shape	65.0	25
			Shape&Csize	62.5	25
	GM – fixed+curve	Track	Csize	26.3	1
			Shape	96.3	10
			Shape&Csize	96.3	10
		Pads	Csize	41.3	1
			Shape	75.0	24
			Shape&Csize	75.0	29
	GM – fixed+curve+surface	Track	Csize	26.3	1
			Shape	96.3	8
			Shape&Csize	96.3	8
		Pads	Csize	45.0	1
			Shape	80.0	36
			Shape&Csize	78.8	36

7.4.1 "Entire track" versus "independent pads"

With the exception of the "Csize" only scenarios (see Section 7.4.2), the maximum accuracies of the algorithms from "track" scenario were consistently higher than the ones from "pads" scenarios. It was confirmed by analysing the trend curves of several scenarios (Figure 27). This implies that the relative position of the pads within the track has a non-negligible effect on the identification of the track positions. We therefore focused the next result analyses on the "track" scenarios only.

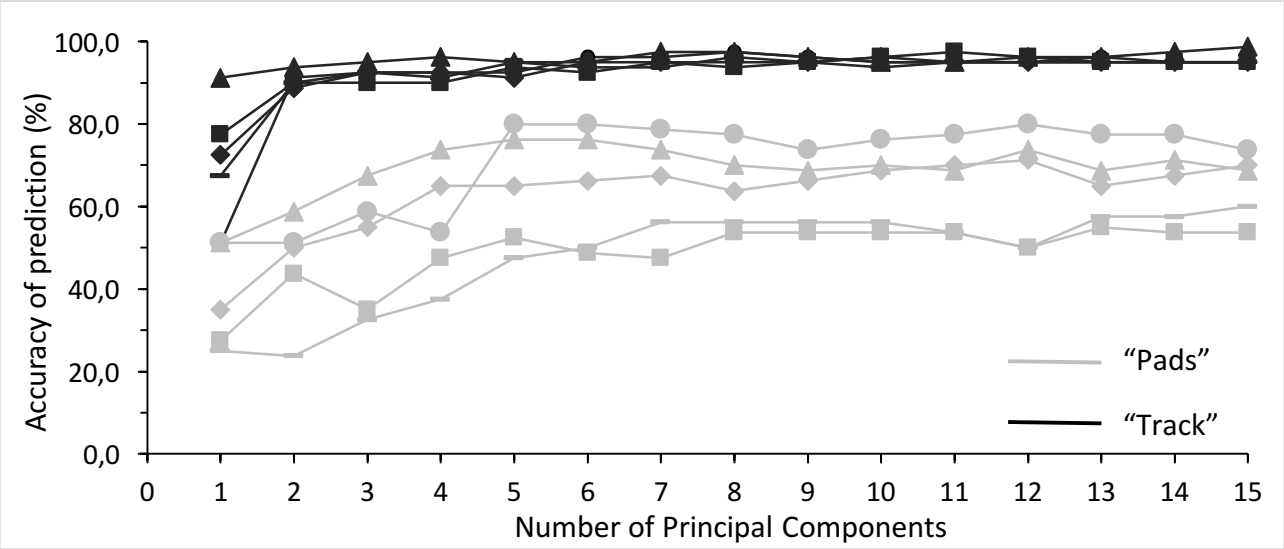

Figure 27 - *Influence of the type of object on the accuracy of prediction of algorithms identifying the track position of spotted hyenas. The line colours represent the algorithms that use information extracted from the tracks (black) or from the "pads" (grey). The shapes of the data points correspond to different scenarios that are compared further in the study: "2D – TM" (circles), "2D – GM – fixed – shape&Csize" (triangles), "3D – GM – fixed – shape" (squares), "3D – GM – fixed+curve – shape" (rhombus), "3D – GM – fixed+curve+surface – shape (dashes).*

7.4.2 Shape and centroid size (Csize)

There was no "Csize" scenario in which the accuracy of the algorithms reaches more than 60% (Table 5). The centroid size alone is therefore unsufficient to identify the position of hyena tracks. However, the identification algorithms happened to procure higher accuracies when the size variable was combined with the principal components of shape (i.e. "Shape&Csize" scenarios). This was the case for "2D – track": the maximal accuracy of the traditional morphometrics scenario ("2D – TM"; in which the information on the size has not been extracted beforehand) was higher than the one that only considered the principal components of the shape ("2D – GM – shape"); but when the size variable was taken into account ("2D – GM – shape&Csize"), the maximum accuracies were among the highest (more than 95%; Table 5). The trend curves left the same impression, especially when less than 6 principal components were taken into account (Figure 28).

In 3D, on the other hand, the maximum accuracies of “Shape” and “Shape&Csize” do not differ between the scenarios that use the same type of landmarks. For instance, the maximum accuracy of “3D – fixed – shape” equals the one of “3D – fixed – shape&Csize”. Same goes for “fixed+curve” and “fixed+curve+surface”. However, the trend curves (Figure 29) indicate that the inclusion of the size variable in the algorithm has a small negative impact: for each given number of PC, the algorithms from “shape&Csize” scenarios gave either the same or a slightly lower accuracy than the ones from the “shape” only scenarios.

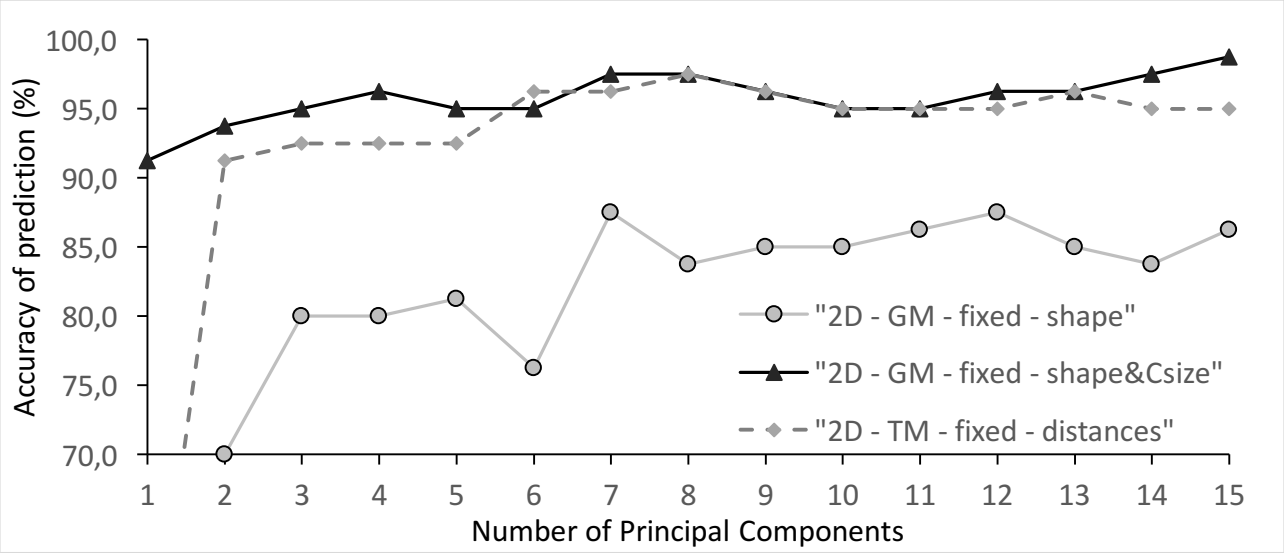

Figure 29 –*Influence of the type of variables on the accuracy of prediction of algorithms identifying the track position of spotted hyenas. The scenarios “shape” (unbroken grey line) and “shape&Csize” (unbroken black line) are compared as geometric morphometrics was applied on the fixed landmarks of their 2D entire tracks. The dashed line represents the corresponding scenario in which traditional morphometrics (TM) was applied.*

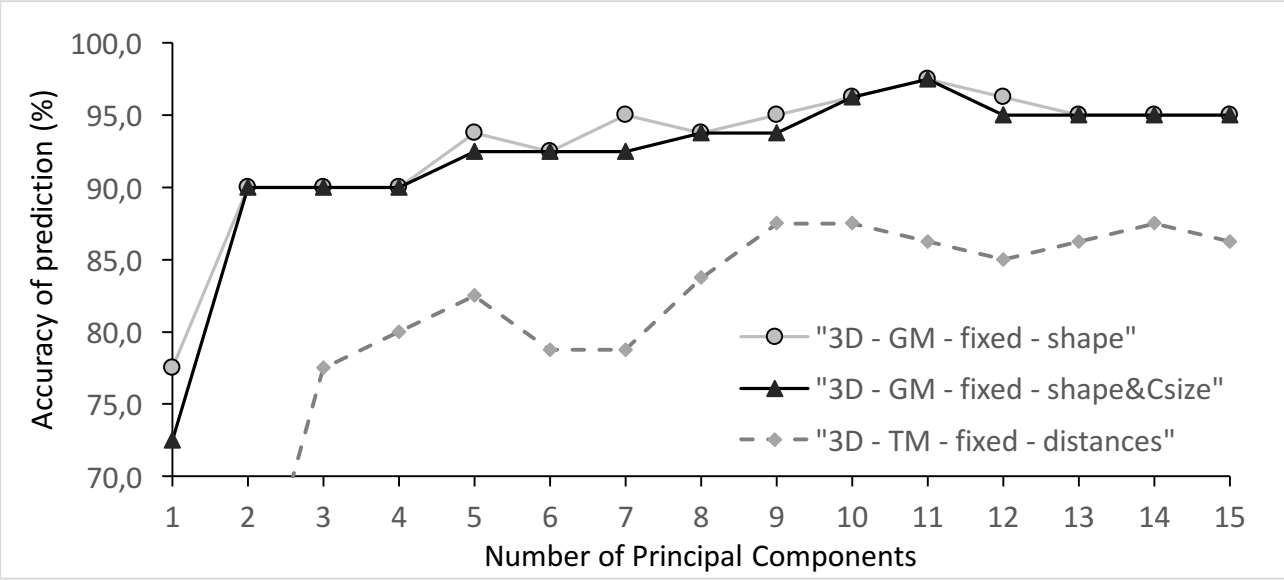

Figure 28 –*Influence of the type of variables on the accuracy of prediction of algorithms identifying the track position of spotted hyenas. The scenarios “shape” (unbroken grey line) and “shape&Csize” (unbroken black line) are compared as geometric morphometrics was applied on the fixed landmarks of their 2D entire tracks. The dashed line represents the corresponding scenario in which traditional morphometrics (TM) was applied.*

7.4.3. Type of model and landmarks

Table 5 indicated that the highest recorded accuracy was 98.8% and belonged to both scenarios “2D – GM – fixed – shape&Csize” and “2D – GM – fixed+curve – shape&Csize”. However, the number of PC they required to reach that accuracy is among the highest too (15 and 10 respectively), which means that their identification algorithms were more complex. With an accuracy of 97.5%, the scenarios “2D – TM” (8 PCs) and “3D – GM – fixed” (11 PCs) come in second place. The “3D – fixed+curve” and “3D – fixed+curve+surface” scenarios, as well as the “2D – fixed+curve – shape”, share the third place with an accuracy of 96.3% and 8 to 10 PCs.

The maximum accuracies of these algorithms are quite close to each other, and require a lot of PC to reach them. Their trend curves were therefore analysed as well (Figure 30).

Whichever the comparative approach that is being used (i.e. limited number of principal components or minimum acceptable accuracy; Section 6.4.5), it is one of the scenario that applied geometric morphometric on 2D-models that provided the most effective algorithms (“2D – GM – fixed” or “2D – GM – fixed+curve”).

Considering the different combinations of landmarks that were used on 3D-models (“fixed”, “fixed+curve”, “fixed+curve+surface”; Figure 30), the scenario that involved the three types all together presented a slight advantage on the two others. For instance, if the number of principal components was limited to 5 or 10, it is its algorithms that would procure the highest accuracies (95.0 and 96.3% respectively). However, if there is no restriction on the number of principal components, the “3D – fixed” scenario obtained the best accuracy of all (97.5%, with 11 principal components).

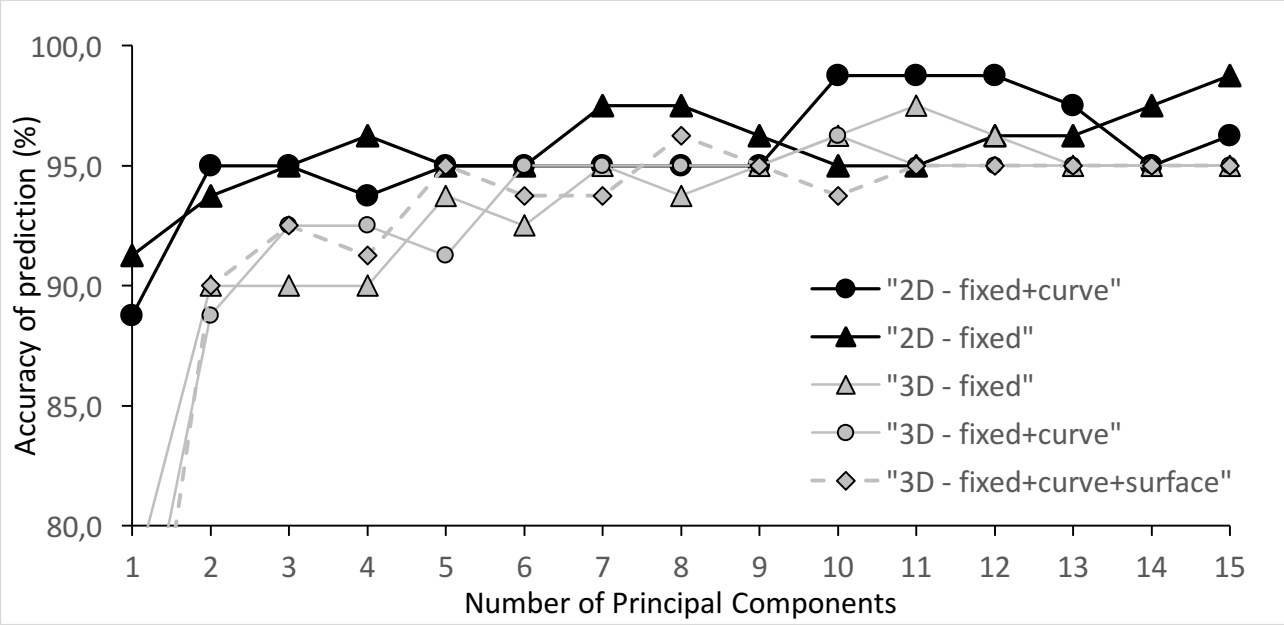

Figure 30 *- Influence of the type of model and type of landmarks on the accuracy of prediction of algorithms identifying the position of spotted hyenas. The colour code represents the type of models: 2D in black, 3D in grey. The shapes of the data points correspond to the type of landmarks used: triangles for fixed only, circles for fixed+curve, diamonds for fixed+curve+surface.*

8 DISCUSSION

8.1 Result interpretation

An entity was defined by (i) a type of model (which was related to the data recording method, i.e. 2D or 3D), (ii) a method of feature extraction (traditional or geometric morphometrics, using fixed landmarks combined or not with curve- and/or surface-sliders), and (iii) a type of object (a "pad" or the entire "track"). For almost every entity, we have obtained at least one position identification algorithm whose maximum accuracy reached 95%. It was therefore difficult to determine if one stood out more than the others by using the "maximum accuracy" as only criterion.

Considering the fact that the complexity of the algorithm increases with the number of variables it takes into account (i.e. the number of principal components), we recommend that the scenario to be chosen should be the one whose algorithm reaches a minimum acceptable accuracy with a minimum number of PCs. That minimum acceptable accuracy is to be decided by the scientists who are in need a position identification algorithm.

In the present study, the scenarios "2D – GM – fixed – track – shape&Csize" and "2D – GM – fixed+curve – track – shape&Csize" provided the best accuracies (more than 95%) with the lowest number of principal components (less than 10) (figure 30, Section 7.4.3).

As already mentioned, several algorithms were created for each entity. Each took into account a type of object ("pads" or "track") and a type of variables (shape components, centroid size, or both) (Section 6.4.5). The importance of the information obtained from each object and variable could then be determined.

8.1.1 Type of object

We first noticed that the accuracies of prediction of the "track" algorithms were substantially higher than the ones of the "pads" (Figure 27, Section 7.4.1). The PCA plots had led to a similar assumption: the two principal components of the "track" entities were enough to segregate the different track positions (Figure 26, Section…), whereas the two principal components of the pads, in spite of higher cumulative proportion of explained variance, were not (Figure 25, Section…). We therefore concluded that the relative position of each pad within a track provides essential information for the identification of the position of that track.

It is now important to remember that the type of substrate has an impact on the shape of a track, but also on the spacing of the pads within the tracks (Liebenberg, 1990): if the soil is slippery, animals tend to spread their toes to better stabilize themselves. In this study, all the considered tracks were sampled in sandy soils along a riverbed, so the variability due to different types of substrate could not be considered. But now that we have pointed out the importance of the relative position of the pads within a track, the influence of the substrate should be studied, in order for the identification algorithms to take it into account. To do so, the variability due to factors other than

soil characteristics has to be limited. For instance, tracks from the same known individuals should be sampled among the different types of substrate that are considered, so that the shape variations of the tracks would be due to the characteristics of the soil and not the morphology of the individuals' paws.

8.1.2 Type of variable

The algorithms that used the centroid size as only variable obtained very low accuracies of prediction (less than 60%), both in 2D and 3D. But when combined with principal components of shape variations (i.e. "shape&Csize" scenarios), the accuracies of the algorithms, when compared to the ones from "shape" only scenario, were higher in 2D and lower in 3D.

These results coincide with the analyses of variance that were conducted on the centroid size distribution of each entity (Table 3, Section 7.2.2): track position had a significant influence on the size of 2D-models (hence the higher accuracies of the algorithm when the "Csize" variable was taken into account by the LDA), but no influence at all on the size of 3D-models (hence the lower accuracies of the algorithm when the "Csize" variable was taken into account by the LDA: it brought in background noise rather than pertinent information). However, this raised the question "how could the influence of track position be significant on 2D-models but inexistent on 3D-models?"

We believe that, in spite of the fact all the tracks were sampled in a similar type of substrate (sandy soil along riverbeds), the variability of the third dimension was too substantial. Because the segmentation (even on coloured tracks) and landmark positioning were quite subjective (Section 8.2), the fixed landmarks and curve-sliders digitized on 3D models were not coplanar: the depth at which the segmentation was made may not have been the same from one pad to another, neither within one same pad. It seems plausible that these variations have created background noise that could have prevented the perception of the influence of track position on the size.

This is quite unfortunate, as the size variable seemed to be an essential piece of information for the identification of the anteroposterior (front or hind) position of the track. Indeed, the fact that front tracks were bigger than hind tracks was already noticed during data recording, and the centroid size does improve the accuracy of the algorithms in 2D. We can imagine that if the size variable had not been such a source of background noise in 3D-models, the "shape&Csize" algorithms of 3D-scenarios could have been more accurate than their "shape" only algorithms, and have therefore competed more with the "2D – shape&Csize" scenarios.

A potential solution to remove depth variability is presented in paragraph 8.3.2.

8.2 Manipulator bias

The results from the LDA indicated that the algorithms identifying track position are more accurate with 2D-models than with 3D's (Figure 30, Section 7.4.3). However, it is also important to consider the manipulator bias that is present in each method, especially during the segmentation process and landmarks digitization. This manipulator bias should be quantified and used as another criterion to compare the different methods that were tested.

8.2.1 Segmentation process

As explained in Section 6.3.1, the pads of a track were often very hard to distinguish from each other and from the intact substrate. Their segmentation from 2D-images was very subjective and probably biased by the fact that the manipulator approximately knew the shape of the track beforehand. If it had not been the case, the variability of the shape of each pad would have probably been more substantial, which could have led to less accurate identification algorithms.

On the other hand, the coloration of 3D-models based on their depth made the contour of the pads more noticeable (Figure 15, Section 6.3.2.2). It is therefore expected that the manipulator bias related to the segmentation process in 3D was considerably lower than the one in 2D. However, the segmentation of 3D-meshes was done manually as well, and the depth at which the pads were to be cut out was not defined beforehand. This step is the most probable source of the variability that led to the "loss" of information on centroid size (Section 8.1.2). A potential solution to reduce the variability that is due to manipulator bias is the automation of the segmentation process, presented in Section 8.3.2.

A method to estimate the manipulator bias of the segmentation step would require several manipulators to repeat the process on a subsample. The surface of the resulting meshes and images could then be measured and their variability calculated; and by conducting an ANOVA, the influence of the type of model and of the manipulator on the surfaces can be tested.

8.2.2 Landmark digitization

The manipulator bias related to the digitization of fixed landmarks can be characterized by the measurement error, which can be tested by calculating the repeatability (Zelditch *et al.,* 2012): with several manipulators repeating the measures (i.e. landmark positioning) on a subsample, a Generalized Procrustes Analysis and Procrustes ANOVA can be conducted to test the influence of the individual objects and repetitions on shape. The repeatability is then calculated using Equation 3 (Zelditch *et al.,* 2012).

$$Repeatability = \frac{Individual\ variance}{(Mean\ Squares_{Repetitions} + Individual\ variance)}$$ Equation 3

With

$$Individual\ variance = \frac{(Mean\ Squares_{Individuals} - Mean\ Squares_{Repetitions})}{Number\ of\ repetitions}$$ Equation 4

In the present study, the influence of 2D or 3D models on the repeatability of landmark positioning could have been tested, but we assumed that the bias encountered during track segmentation would have been reflected in the results. Therefore, comparing the variability resulting from the segmentation process in 2D and 3D seemed more suitable to assess which type of models is less prone to manipulator bias.

8.3 Automation of modelling process

To apply a more efficient modelling process both in term of time and manipulator bias, methods to automate its different steps should be investigated. In this section, we give a couple of ideas to start with.

8.3.1 Scaling of 3D-models in *Photoscan*

To provide a scale to the models of the tracks, square rulers were positioned around the tracks (Section 6.2). The markers used to create the scale bar in *Photoscan* had to be manually positioned (Section 6.3.1.1), which made the process quite time consuming and, in spite of the projection of predictor rays by Photoscan on a second image, prone to manipulator bias.

For future studies, we therefore recommend the use of automatic targets instead. By positioning them on the square rulers (Figure 31), the scaling process in *Photoscan* can be automated on every model sequentially (Agisoft help desk).

Figure 31 – *Automatic targets placed on a square ruler during data recording. They allow the automation of the scaling process of the models in Photoscan.*

A similar automation process might be possible for 2D-models, but a software capable of doing so was not found at this time.

8.3.2 Segmentation process

Because of the lack of contrast between the track and intact substrate, automatic segmentation on 2D-images is very likely impossible. It may be possible to enhance that contrast by using more sophisticated lighting during data recording, and to obtain a better image quality by stabilizing the camera on a tripod (which, by being placed directly above the track, would also limit the risk of parallax error). However, these techniques would require (i) extra material to carry around (instead of just a camera and square rulers), (ii) extra time to position these materials (which is not ideal, considering the danger one can face in the wilderness), and (iii) a manipulator with relatively good photographing skills (which would limit the number of citizen scientists capable of collecting data).

In *CloudCompare* (the software used for segmenting 3D-meshes), a solution to standardize the depth of the meshes could be possible. Once the track is aligned such as its depth is defined by the z-axis (Figures 14 and 32), it should be possible to cut the track with a plane that is perpendicular to the z-axis (i.e. to the depth). The intersected curve could then be used to digitize curve-sliders, and the planarity of the landmarks could be ensured, hence reducing the variability of the z-coordinates.

However, the shape of a pad tends to vary with its depth: a pad that is segmented at different depths will result in boundary curves of different shape. Defining the depth at which the track should be horizontally cut (i.e. the equation of the plane) is therefore another source of variability that has to be considered. To prevent this bias, we recommend that the depth of the mesh (i.e. the distance from the plane to the deepest zone of the track) is to be the same for each pad. To do so, the equation of the plane should be of the same form as Equation 5, in which “h” equals the initial depth of the pad (before segmentation), and “d” the depth that all the segmented pads would have in common after segmentation.

$$z = -h + d \qquad \text{Equation 5}$$

Note that the plane “z = 0” would correspond to the surface of the intact soil surrounding the track, and “z = -h” the plane tangent to the deepest surface of the pad (Figure 32).

The depth variations between the 3D-meshes would therefore be non-existent, which implies that (i) the surface-sliders would describe the shape variation of the lower surface of the pads only, without being influenced by the global depth of the track, and (ii) the information on the Centroid size might not be lost.

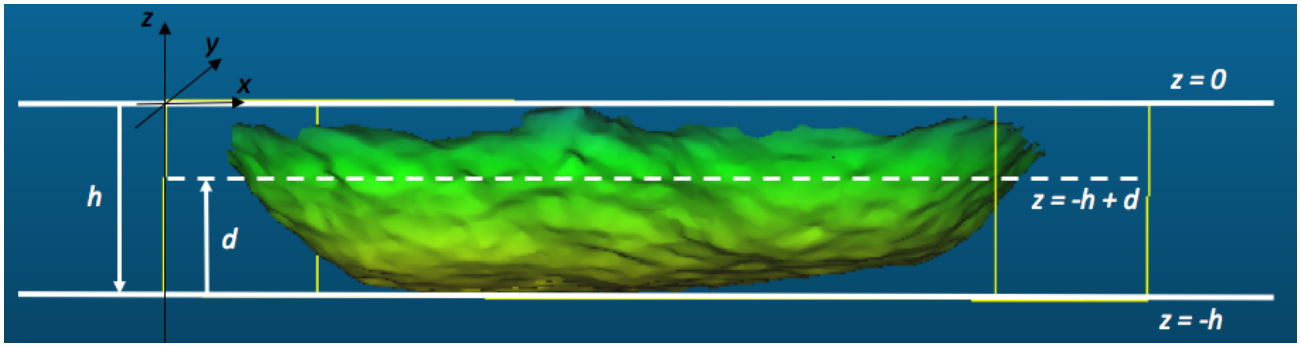

Figure 32 – *Schematic of the horizontal segmentation of a main pad in order for the resulting mesh to have a given depth. "h" represents the initial depth of the pad; "d" represents the depth of the final mesh of the pad, which is common for all the other pads of the dataset. The equation "z = 0" corresponds to the surface of the intact soil surrounding the track. The equation "z = -h" represents the plane tangent to the deepest surface of the pad. "z = -h + d" is the equation of the plane cutting the track in order for the depth of the resulting mesh to be equalled to d.*

8.4 Accuracy of prediction of the algorithms

As explained in Section 6.4.5, the accuracy of prediction of an algorithm can be calculated by conducting either a LDA with or without jack-knife. A third approach can be investigated: the algorithms can be tested on an independent dataset of tracks. Their accuracy would equal the number of track correctly identified divided by the total number of track present in the independent dataset.

8.5 Number of principal components

The choice of the number of principal components used by the algorithms could have been less subjective by conducting a MANOVA, such as the Pillai's Trace test (Andale, 2016). Its value, ranging from 0 to 1, indicates the discriminating power of each variable used by the algorithm, i.e. it indicates how valuable a variable is for the identification of the position of a track. Removing the variables whose Pillai values are under a certain threshold could have decreased the background noise that the LDA may have encountered, resulting in a lower error rate (i.e. higher accuracy of prediction of the algorithms).

Instead of conducting LDA with an increasing number of PC, the first algorithm to be created would involve all of the PC originating from the PCA. The Pillai's Trace test would then attribute a value to each PC. The PC that obtain a value lower than a given threshold (0.5 for instance) would be discarded, while the others would be taken into account by the next algorithm to be constructed.

9 CONCLUSION

Out of 31 tested algorithms, 9 were able to distinguish the anteroposterior (front or back) and mediolateral (left or right) position of spotted hyena tracks with more than 95% accuracy. Two in particular, from the combinations of methods "2D – GM – fixed – track – shape&Csize" and "2D – GM – fixed+curve – track – shape&Csize", showed successful identification in 98.8% of the tested tracks, while the algorithm from "3D – GM – fixed – track – shape" acquired an accuracy of prediction of 97.5%, which is more than that tested on lion tracks (91.2%; Marchal *et al.*, 2017). However, this comparison is biased as the tracks were not characterized by the same number of landmarks (19 for hyenas and 12 for lions). It would therefore be interesting for future studies to analyse the influence of the number of fixed landmarks used to characterize a track on the accuracy of prediction of the identification algorithms.

The relative position of the pads within a track seems to provide information that was essential for the identification of the position of a track. This is not surprising, considering that experienced trackers usually look at the position of the "little toe" (i.e. the homologue of our little finger) to determine right from left (WWF-India, 2005).

As the front tracks were significantly bigger than the hind ones, the size variable (i.e. the centroid size in geometric morphometric) also brings essential information to the identification algorithm, but it was not sufficient to discriminate the four track positions by itself. It is therefore the combination of both shape and size variables that should be considered (instead of each independently from one another). As a consequence, the use of a ruler during sampling is necessary to include the size-information in the model.

Before being able to establish which type of model (2D or 3D) and which type of landmarks (fixed only, fixed and curve-sliders, or fixed and curve- and surface-sliders) provide the most accurate algorithm, the manipulator bias of each method has to be quantified and used as a second evaluation criterion. The track modelling process (both in 2D and 3D) also needs to be made more effective both in term of time and manipulator bias. To do so, the automation of the different steps involved should be investigated.

In spite of these few improvements to be made, the results of the present study are already very promising, as the accuracies of prediction of several algorithms have exceeded 95%. The use of algorithms capable of identifying track position should therefore be extended to other species, as it has already been done by Marchal *et al.* on lions (2017). The objective identification of track position should improve the reliability and efficiency of wildlife monitoring studies worldwide. For instance, in the case of a study that involve the identification of species or individuals from their tracks, the manipulators need to ensure that the compared tracks are from the same anteroposterior and mediolateral position, in order (i) to prevent over-estimations of a population, such as the one the pugmark census method led to (Karanth *et al.*, 2003), and (ii) to decrease the risk of misidentifying a known individual because the newly-sampled track does not correspond to the one previously recorded. Also, algorithms identifying track position will enable a more objective description of trails. When different individuals move with the same gait under the same conditions, trail variables,

just like tracks, provide information that may be useful to the identification of certain behaviours and biological characteristics (Marchal, 2017). Every individual (or category of individuals, i.e. male/female, young/old) has a particular gait, whose variations may be perceptible in the track positions within their trail (Liebenberg, 1990). But to compare trail variables between different (groups of) individuals, the measures recorded between the tracks must be homologous. For instance, the right pace (i.e. the distance between the front right and hind right tracks) of an individual cannot be compared to the left pace (i.e. the distance between the front left and hind left tracks) of another. This can be ensured by identifying the position of tracks from their models with the type of algorithm created in the present study.

This study, along with the ones conducted by Marchal (2017), shows that the use of tracks and trails as a monitoring technique is a reliable alternative to the current invasive and expensive ones. It does not require the capture or even the sighting of the monitored individuals, and the cost is limited to a camera for the sampling protocol and the software used for track modelling (Photoscan and Rhinoceros). Furthermore, the simplicity of the sampling protocol and the commercially available equipment that is required (camera and square ruler) could enable citizen-scientists and community members to get involved in the research by collecting data. By then sending photographs to a research team (e.g. through the use of an online platform for instance) a large database could be rapidly constituted and used by a third party to conduct the 3D-processing steps, feature extraction and statistical analyses.

“Unless we can allow not only elephants, but all the wild animals their place in the sun,

We can never be whole ourselves”

- Lawrence Anthony